FINAL REPORT

Research Project B-509

CHEMICAL REACTIVITY OF HYDROGEN, NITROGEN AND OXYGEN ATOMS AT TEMPERATURES BELOW 100°K

by

Henry A. McGee, Jr.

NASA Grant NGL-11-002-005 (formerly NsG 337)

August 1973

Performed for

National Aeronautics and Space Administration
Planetary Programs Office
Washington, D.C.

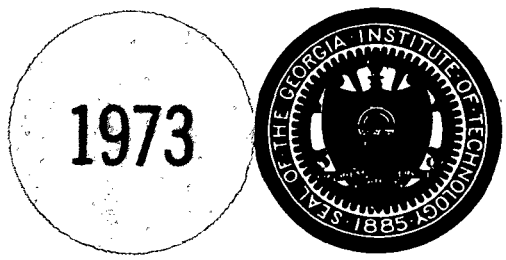

School of Chemical Engineering
GEORGIA INSTITUTE OF TECHNOLOGY
Atlanta, Georgia

CHEMICAL REACTIVITY OF HYDROGEN, NITROGEN, AND OXYGEN ATOMS AT TEMPERATURES BELOW 100°K

Final Technical Report

on

Grant NGL-11-002-005

National Aeronautics and Space Administration

Planetary Programs Office

Washington, D. C. 20546

ABSTRACT

This research has been concerned with the synthesis of unusual compounds by techniques employing cryogenic cooling to retard their very extreme reactivity. Examples of such species that were interesting in this program are diimide (N_2H_2), cyclobutadiene (C_4H_4), cyclopropanone (C_3H_4O), oxirene (C_2H_2O), and many others.

New and generally applicable analytical techniques using the mass spectrometer were developed. These instrumental adaptations permitted the qualitative and rough quantitative analysis of compounds such as the above. Special purpose cryogenically cooled inlet arrangements were designed such that the analyses incurred no warm-up of the cold, and frequently explosively unstable, compounds. Controlled energy electron impact techniques were used to measure critical potentials and to develop the molecular energetics and thermodynamics of these molecules and to gain some insight into their kinetic characteristics as well.

Three and four carbon strained ring molecules have been studied. Several reactions of oxygen and hydrogen atoms with simple molecules of H, N, C, and O in hard quench configurations have been studied. And the quench stabilization of BH_3, though of little astrophysical interest, has been explored as a model system in cryochemistry. Unfortunately, the species could not be prepared as a stable cryochemical.

This research program was initiated on January 1, 1966 and terminated on June 30, 1971 when the principle investigator moved to Virginia Polytechnic Institute and State University. The research formed the doctoral theses of five students and the masters thesis of one student. The program was continued at VPI&SU under grant NGR 47-004-080 effective July 1, 1971.

TABLE OF CONTENTS

CHAPTER I

INTRODUCTION AND BACKGROUND INFORMATION

This research program has been concerned with the development of chemical information at cryogenic temperatures, particularly on systems that astronomers and astrophysicists feel are important in comets and in the atmospheric and surface chemistry of the Jovian planets. Each of these astronomical objects is very cold, and clearly insofar as chemistry plays a role in the behavior of these objects, that chemistry must be occurring at very low temperatures by terrestrial standards. This objective rather quickly resolves itself into studies of low molecular weight compounds of the four elements of maximum cosmic abundance, namely hydrogen, carbon, nitrogen and oxygen.

The approach here is not one of free radical stabilization, i.e., centered upon attempts to isolate labile species in inert matrices at very low temperatures. All evidence suggests that the activation energy for the reaction of low molecular weight free radicals is zero (or close to it), and hence it will be possible to prepare these species in "stable" forms only by such diffusional inhibition techniques. The resulting concentrations of labile species are limited to a maxiumum of a few tenths of a per cent (usually much less), and hence the importance of such systems in cosmic chemistry would seem to be minimal. The matrix technique, particularly when combined with ir or epr instrumentation, does, of course, provide a powerful means to study the physical and chemical properties of free radicals.

By contrast, low molecular weight labile species which have singlet electronic ground states, i.e., species that are highly reactive but are not free radicals, are in an altogether different category. Examples of such substances are cyclobutadiene, cyclopropanone, oxirene, diimide, ammonium ozonide, benzyne, tetrahedran, and many others. One would expect

such species to exhibit an activation energy for reaction, but we would also expect this energy to be unusually small. If an activation energy exists, then substances such as these may be preparable as stable cryochemical reagents and a true chemistry at a very low temperatures may be developed. Since the activation energies involved in these systems are small, it will usually be necessary to maintain the compounds below some critical temperature if they are to be manipulated as stable, pure reagents. Hence, new cryogenic manipulative techniques had to be developed, for ideally one must transpose all of the common or usual operations of bench scale chemistry to permit their convenient utilization at cryogenic temperatures. The most important operation in any chemical investigation is analysis. Several unique cryogenically cooled reactor-inlet attachments to the time-of-flight mass spectrometer have been developed under this grant. The cryogenic mass spectrometer has proven to be an efficient analytical tool in low temperature chemistry.

The best characterization of those strange nomads of space, the comets, is the so-called "dirty snowball" model of Whipple as modified by Donn and Urey.[1] Here the comet's nucleus is considered to be composed of frozen ices of simple compounds such as H_2O, NH_3, H_2O_2, C_2H_2, etc., and some meteoric dust. However, it has been necessary to postulate highly energetic reactions occurring at very low temperatures in order to explain some of the cometary phenomena that are observed by astronomers. It is possible, if not highly probable, that these reactions involve as yet unknown species which are stable when cold but which react vigorously upon slight warming. The search for the existence of such species and the study of their chemistry and energetics was one of the primary objectives of this NASA research program. Other than the comets, the atmosphere and surfaces of the Jovian planets are also very cold (even Mars is much colder than earth), and hence the equivalents of earthbound meteorology, geochemistry, and possibly other areas of geophysics in which chemistry is important, must be understood, as it applies to that particular planet, in terms of low temperature chemistry. A build-up of general knowledge in the phenomenological chemical behavior of species likely to be present in such environments will be valuable inputs to the engineering designs of landing vehicles for both manned and unmanned explorations of the future.

As this work has developed, we have found rather eager interest on the part of segments of the chemical process industry in many of these same sorts of reactions. These people are interested in energy storage and conversion and in chemical synthesis. Our way of life depends upon the inexpensive availability of a wide variety of chemicals in tonnage quantities, and any process or technique which offers hope of economy or variety in these syntheses is sure to attract attention. The low temperature procedures developed here represent a totally new dimension of preparative chemistry, and since industrial chemistry is preparative chemistry, they also represent new dimensions (however embryonic) of industrial chemistry. This broad interest in developing such a new dimension of industrial chemistry in addition to the above enumerated areas of application in space chemistry, have formed the objectives of this program.

Accomplishments under this grant have been in the areas of (1) instrumentation development, (2) the development of phenomenological chemical information at cryogenic temperatures, (3) the energetics of low molecular weight, highly unstable and reactive molecules which have been synthesized by cryochemical procedures, and (4) in the training of doctoral students. The details of accomplishments in these several areas have been presented in a series of semi-annual progress reports and in a series of reprints of journal articles and theses which have from time to time been forwarded to NASA as they were published. These details will not be enumerated here. It is, however, appropriate to include a capsule resume of the completed research.

CHAPTER II

RESEARCH RESULTS - EQUIPMENT DEVELOPMENT

Before chemistry at very low temperatures will progress very far, the common operations of bench scale experimentation must be translated to the point of convenient utilization at cryogenic temperatures, and perhaps the most fundamental operation of all is that of chemical analysis. The analytical facility that was invented during this program was designed for the study of the synthesis, stability, reactivity, and energetics of that interesting class of compounds which usually must be synthesized and maintained below some rather low temperature if the compound is to exist as a stable entity or chemical reagent. Examples of such compounds that are either known or pseudo-known are H_2O_3, H_2O_4, BH_3, HNO, NO_3, N_2H_2, NH_4O_3, etc. Manipulations with these species must be conducted at temperatures below the onset of that loss process having the lowest activation energy, and this may be $100^{o}K$ or lower.

A. General Design Considerations

Both the synthesis reactions and the subsequent studies of the reactivity and energetics of the species of interest must be conducted in cryogenically cooled systems. Experience has shown that simple transfer operations such as pipetting, liquid flow, or vaporization and recondensation become difficult operations when the working substance is thermally unstable at cryogenic temperatures. Also the purification techniques that might be applicable to such systems are complicated by the temperature requirement, and hence each will require development prior to its use. Therefore, it was desirable to combine into one device, insofar as it was possible, the features of a versatile chemical reactor, some capability for separative operations, and chemical analysis by mass spectrometric means.

Almost without exception, reactions which proceed at cryogenic temperatures involve at least one reactant which is a free radical and which is usually generated by electric discharge, pyrolysis, photolysis, or by chemical reaction (such as a low pressure flame). So the experimental arrangement should also be versatile enough to reasonably accommodate these several free radical generation operations.

The mass spectrometer was selected as the primary analytical device for these investigations because, unlike electron spin resonance

or infrared, which have both been widely and successfully used in related experiments, the mass spectrometer detects all species. It also affords a direct observation of the species of interest and the output data require a minimum of equivocal interpretation. Very small quantities are adequate for analysis. An identification may be obtained in the present system provided only that a species exert a vapor pressure of about 3×10^{-6} torr and that the vapor will, upon electron impact, give a sufficient intensity and variety of either positive or negative ions having a lifetime at least of the order of 50 microseconds. The identification is also aided by the use of an ionizing electron beam of controlled energy, and by the control of the temperature of the inlet system which takes advantage of the relative volatility and hence the separability of the several components that may be present from a particular experiment. The open structure of the source of the Bendix spectrometer, which makes it possible to assemble complex hardware adjacent to and even within the source itself, was the deciding factor in the selection of that machine. Many other adaptations of the TOF instrument in situations where this open source structure has been advantageous have been recently summarized.[2] The disadvantages of the TOF instrument stem from the low duty cycle of 0.005 which results from its control pulse of 0.25 microseconds at a frequency of 20 Kc, i.e., the machine is effectively off 99.5 per cent of the time. The only earlier mass spectrometer adaptation that seems reasonably related to the present arrangement was described by Blanchard and LeGoff.[4] In their apparatus, the walls of the ionization chamber were cooled with liquid nitrogen, and the system was employed in unsuccessful attempts to condense and revaporize I atoms.

The innovation of cryogenic mass spectrometry is described in some detail below. But the system could be viewed in some sense, as rather similar to a heated filament inlet system for use with the Bendix instrument that was developed by Biemann[3] and in which termally sensitive organic substances contained in a tiny capsule may be positioned inside the source adjacent to the ionizing electron beam of the instrument. Heating the capsule produces vaporization directly into the electron beam, and hence there are few collisions and therefore little reaction or degradation before ionization. Our system is similar, but it operates at the far opposite end of the temperature spectrum.

B. Mechanical Description

A schematic of the apparatus appears in Figure 1 where the reactor-inlet system is shown in operating position near the electron beam. The reactor-inlet system is suspended from a vacuum header and consists of a thermostated refrigerant chamber made of copper for rapid thermal equilibration which was nickel plated on the outside to reduce the emissivity and hence the refrigerant use rate. The monel reactor and condensation tube in which the low temperature species are prepared and manipulated is inside this refrigerant chamber. Thermostating is accomplished by offsetting the natural inward heat leak with a controlled influx of refrigerant which is adjusted to be slightly in excess of that required to just balance the natural heat leak. Fine control is then maintained automatically by a recorder-controller (Leeds and Northrup Company, Adjustable Zero-Adjustable Range-Speedomax H) which controls the power dissipated in 100 ohm constantan heaters wound on the inside of the chamber. Electrical trimming of the heat balance can be much more precisely controlled than is possible with flow control of the liquid refrigerant. Proportional control of these heaters was not required since simple two-position operation resulted in oscillations about the control point which increased to a maximum of only $\pm 0.5^{\circ}K$ when the apparatus was cooled to near $77^{\circ}K$.

A gas pressurized refrigerant delivery system maintains the flow of liquid N_2. Close control and monitoring of the influx of refrigerant is accomplished by adjusting a micrometer valve until the desired flow rate is attained as indicated by a flowrator in the frigerant chamber exhaust line. From the measured vented gas flow rate, one can immediately deduce the liquid refrigerant use rate.

The end of the condensation tube nearest the source is fitted with any one of several flat extension pieces which are positioned to protrude into the ionization chamber of the spectrometer when an analysis is being performed; a channel in this extension piece conducts the sample from the condensation tube into the ion source. The inlet port itself (0.089 cm dia.) may be positioned at any point relative to the electron beam including its being actually submerged in the beam, and hence the cold gaseous sample emerges from the inlet tube directly into the ionizing electron beam, and ionization of the sample occurs prior to any wall collisions. A sample molecule must be considered to be background after

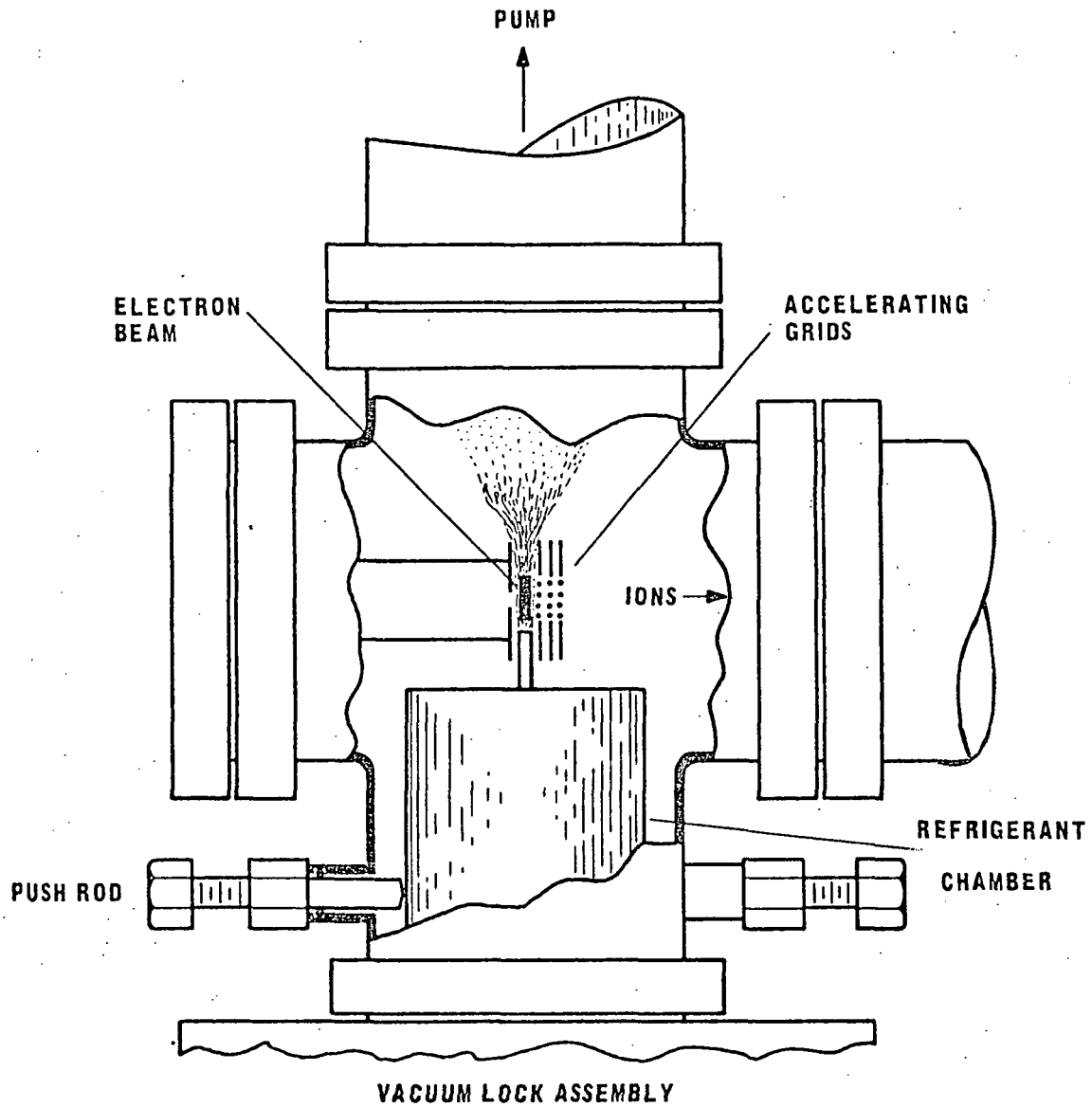

Figure 1. Top view of the "Cross" vacuum chamber of the TOF mass spectrometer which contains the source structure and which is depicted with the cryogenic reactor-inlet system in analytical position.

only one such wall collision. Design calculations, which were confirmed subsequently by experimental measurements, show that the 0.4 x 1.6 cm cross section of the nickle plated copper extension piece provides sufficient conductivity along its 2.5 cm length to insure that the sample is not heated significantly above the temperature of the refrigerant chamber when it passes through the inlet channel. The maximum calculated ΔT was $0.8^{o}K$ and the measured value was somewhat less than $2^{o}K$. The difference was probably due to the thermal resistance at the solder joint where the extension piece joins the refrigerant chamber. These ΔT's were however quite acceptable. The lateral positioning of the reactor inlet device is accomplished with a screw, and an observation port is provided to visually follow the advance of the extension piece into the ion source structure. Sidewise positioning adjustments in the plane perpendicular to that of Figure 1 are made during this advance by a pair of oppositely placed, vacuum sealed push rods which are mounted on the "cross" vacuum chamber. This rather delicate alignment situation is apparent in Figure 1. Fast pumping in the source region is provided by a nominal 750 l/sec system. The reactor-inlet system passes through a vacuum lock arrangement so that the system can be withdrawn for adjustment without the necessity of breaking the vacuum in the mass spectrometer.

C. Ion Source Collision Dynamics

Maximum detectability corresponds to the observation of usable spectra at the lowest sample pressures, hence at the lowest temperatures of the condensed samples that are of interest here, and therefore in the region of greatest thermal and chemical stability of these rather labile compounds.

As originally developed by Clausing[5], it is possible to calculate the intensity of molecules effusing into a vacuum from a circular inlet port of area πr^2 which has some particular ratio of length to radius, L/r. The molecular intensity, N_θ at any solid angle, $d\omega$, located at some angle, θ, with respect to the center line of the port (see Figure 2), may be developed in the form of the cosine distribution function multiplied by a deviation factor, J, which is a complicated function of L/r and θ,

$$N_\theta = [(N_t/\pi)(\cos\theta)(d\omega/dA]J \qquad (1)$$

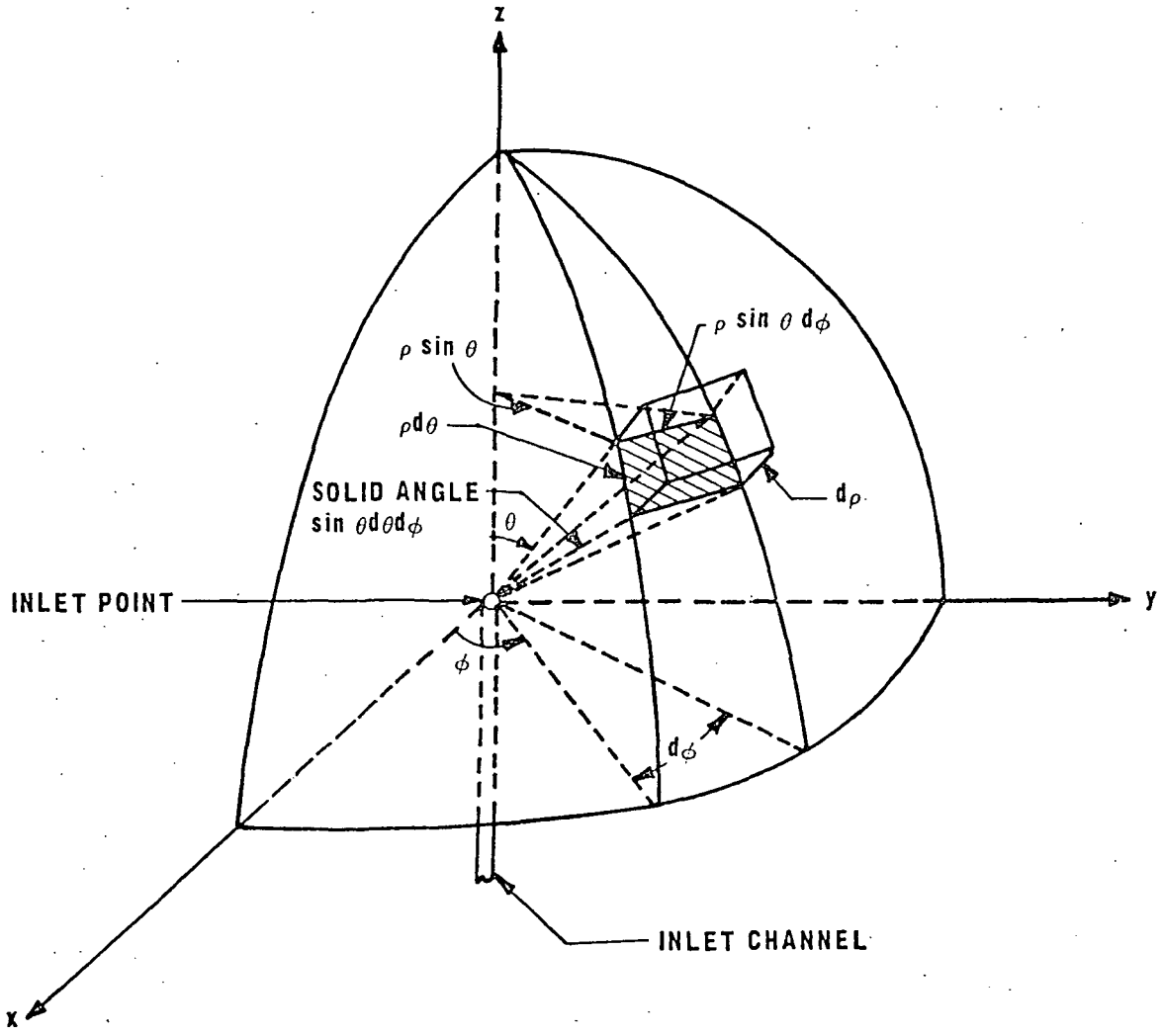

Figure 2. Spherical coordinate system for calculating the number density of molecules at any point, (ρ, θ, ϕ), for the efflux of a gas through a hole in a thin edge orifice.

From the variation of J with L/r and θ[5], it is evident that both the intensity at any angle and the total flow will be a maximum for a sharp edge orifice for which case J has its maximum value of unity. N_t is the rate at which molecules enter the sample inlet channel and is given by the product of the molecular number density in the sample reservoir, the average molecular speed, and the inlet area, i.e., by $PA/(2\pi mkT)^{1/2}$. We are concerned, of course, with the ionization of molecules which have suffered no collisions since leaving the inlet port. The sensitivity, S, is directly proportional to the number of these molecules that are ionized per unit time which is given by the product of the electron flux, N_e, the molecular or the target number density, D(x,y,z), and the ionization cross section, σ_i. Considering the case for which the cosine distribution of intensities is correct, i.e., J = 1 or a sharp edge orifice, the number of molecules emitted per unit of time through the shaded solid angle, $d\omega$, shown in Figure 2 is $N_{t\theta}d\omega$ where $d\omega = \sin\theta d\theta d\phi$. Hence, the molecular flux at that point is given by $N_{t\theta}(d\omega/dA)$ where $dA = \rho^2 \sin\theta d\theta d\phi$. The number density of molecules, $D(\rho,\theta)$, at any point is given by the molecular flux divided by the average molecular velocity,

$$D(\rho,\theta) = (N_{t\theta}\sin\theta d\theta d\varphi)/(\bar{v}\rho^2\sin\theta d\theta d\varphi) \qquad (2)$$

which reduces to

$$D(\rho,\theta) = \frac{N_{t\theta}}{\bar{v}\rho^2} \qquad (3)$$

and since $N_{t\theta} = N_t\cos\theta/\pi$,

$$D(\rho,\theta) = \frac{N_t}{\pi\bar{v}\rho^2}\cos\theta \qquad (4)$$

Equation (4) gives the number density of molecules at any point in spherical coordinates and corresponds to Equation (1). Transforming Equation (4) into rectangular coordinates yields the expression

$$D(x,y,z) = \frac{N_t}{\pi\bar{v}} \cdot \frac{z}{(x^2 + y^2 + z^2)^{3/2}} \qquad (5)$$

Since the probability that a given molecule will be ionized during a single pass through the electron beam is very small, it can be assumed that the number of target molecules is undiminished as a result of ionization and is therefore correctly represented by Equation (5). The sensitivity, S, becomes,

$$S = K \int_{covol.} Ne\ \sigma_i\ dN(x,y,z) \tag{6}$$

where

$$dN(x,y,z) = D(x,y,z)\ dV(x,y,z) \tag{7}$$

and N_e and σ_i are the electron flux and ionization cross section, respectively. Figure 3 illustrates the general rectangular effective collision covolume of the electron beam of cross section, 2a x 2b and length, $(c_2 - c_1)$, where c_1 and c_2 are the perpendicular distances from the inlet port to the nearest and far faces of the beam, respectively. Assuming that σ_i and N_e are constants and using Equation (5) and (7), Equation (6) can be written, using symmetry properties, as

$$S=(4N_tN_e\sigma_iK/\pi\bar{v}) \int_o^a \int_o^b \int_{c_1}^{c_2} [z/(x^2 + y^2 + z^2)^{3/2}]dxdydz \tag{8}$$

After some manipulations, this equation can be integrated to yield,

$$\begin{aligned} S = \{ 4N_tN_e\sigma_iK/\pi\bar{v}\}\{ & a\ \ln[\gamma_2(b+\beta_1)/\gamma_1(b+\beta_2)] \\ & + b\ \ln[(\alpha_2+\beta_2-a)(\alpha_1+\beta_1+a)/(\alpha_2+\beta_2+a)(\alpha_1+\beta_1-a)] \\ & + c_2\tan^{-1}(a/c_2) - 2c_2\tan^{-1}[ac_2/(\alpha_2+b)(\alpha_2+\beta_2)] \\ & + 2c_1\tan^{-1}[ac_1/(\alpha_1+b)(\alpha_1+\beta_1)] - c_1\tan^{-1}(a/c_1)\ \} \end{aligned} \tag{9}$$

where, $\alpha = (b^2 + c^2)^{1/2}$; $\beta = (a^2 + a^2)^{1/2}$; $\gamma = (a^2 + c^2)^{1/2}$; and where the factor, J, has been taken to be constant and equal to its maximum value of unity. Equation (9) predicts the approximate number of molecules ionized per unit time with the near face of the electron beam a distance c_1 away from the sample inlet port for the case where (1) the flow out of the inlet channel is molecular, (2) the inlet channel is a thin edge orifice, i.e., cosine distribution of intensities from the inlet port, (3) the axis of the inlet channel is aligned with the center axis of the electron beam, and (4) the inlet port is approximately a point source.

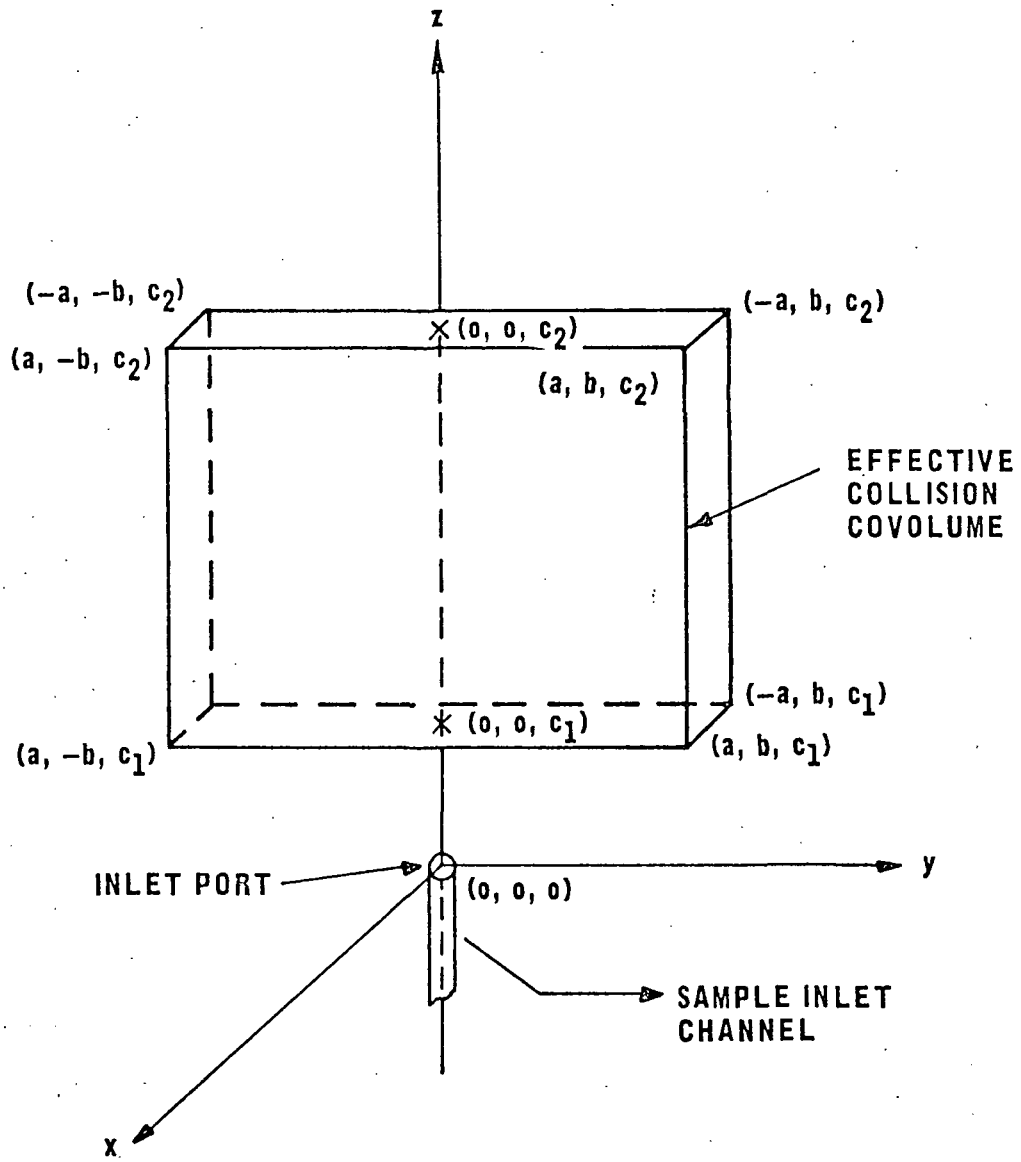

Figure 3. Rectangular coordinate system for integrating over the effective collision covolume to determine the total sensitivity for a given position of the inlet port relative to the electron beam.

For the perpendicular arrangement of the inlet port relative to the electron beam, the geometical parameters in the Bendix source structure, a, b, and $(c_2 - c_1)$, are 0.038 cm, 0.318 cm, and 0.50 cm, respectively. For the coaxial arrangement these parameters are 0.25 cm, 0.318 cm, and 0.076 cm, respectively. Substitution of these values into Equation (9) for various values of c_1 gives the variation in sensitivity for the two arrangements as a function of the distance of the sample inlet port from the electron beam. The factor $S\bar{v}/N_t N_e \sigma_i K$ (more conveniently written $F\bar{v}$) was computed from Equation (9) for both the perpendicular and coaxial arrangements for values of c_1 between $c_1 = 0$ and $c_1 = 3.0$ cm at intervals of 0.005 cm. Some of the values of this factor are tabulated in Table I. $F\bar{v}$ is equivalent to the fraction of molecules effusing from the inlet port per unit time that appear in the effective collision covolume of the electron beam multiplied by the average molecular speed (i.e., $N_b\bar{v}/N_t$) where N_b is the number of molecules in the collision covolume. The paramount importance of minimizing the distance between the inlet port and the electron beam is clear, for if the inlet port is only two mm away from the beam, the sensitivity is down by a factor of four for the perpendicular case. From Table I it was concluded that both the perpendicular and coaxial arrangements provide about the same sensitivity at equal displacements from the near face of the electron beam. These predicted trends have been experimentally verified; e.g., moving the inlet port about 6 mm away from its optimum position results in sensitivity losses of an order of magnitude.

The major deductions from these results were: (1) that the coaxial arrangement and the perpendicular arrangement are equivalent so far as sensitivity is concerned, and (2) the investigation of species that are destroyed in a single collision should be performed with the sample inlet port as close as possible to the electron beam, within less than 3 mm if possible. In view of deduction (1), and the mechanical conveniences discussed earlier, it was concluded that the perpendicular arrangement was preferable to the coaxial arrangement, and the system was designed in that way.

The sensitivity for a stable species also decreased appreciably as the distance of the inlet port from the electron beam was increased, despite the fact that, unlike the cryochemical species, there is an appreciable background due to the stable species. A stable CO_2^+ ion current from CO_2 was observed, and the variation of this current with distance of the inlet

TABLE I. Variation of Sensitivity with Relative Configuration of Electron Beam and Inlet Port

Configuration	Geometrical Parameters (cm)				$\bar{v}F^*$ (from Eq. (9))
	a	b	c_1	c_2	
Perpendicular Arrangement	0.038	0.32	0.0	0.5	0.156
	0.038	0.32	0.2	0.7	0.0387
	0.038	0.32	0.8	1.3	0.0070
	0.038	0.32	1.4	1.9	0.0028
	0.038	0.32	2.0	2.5	0.0015
Coaxial Arrangement	0.250	0.32	0.0	0.076	0.134
	0.250	0.32	0.2	0.276	0.0594
	0.250	0.32	0.8	0.876	0.0087
	0.250	0.32	1.4	1.476	0.0036
	0.250	0.32	2.0	2.076	0.0018

*F is the fraction of molecules entering the inlet channel per unit time that appear in the collision covolume and is equivalent to $S/\sigma_i N_t N_e K$. Maximum detectability with respect to the relative configuration of the electron beam and the inlet port corresponds to a maximum value of F.

port from the electron beam was studied. Figure 4 illustrates the variation that was obtained. It can be seen that the intensity decreases by a factor of about 13 when the inlet port is moved from its optimum position, where the electron beam is in grazing incidence, to a distance about 2.5 cm away from the near edge of the electron beam. This is an order of magnitude less than the factor of about 150 indicated from Table I for an unstable species, i.e., with no allowed background sample, but the decrease still represents a considerable loss of sensitivity.

The above calculations are for the case where the inlet port is a thin edge orifice which corresponds to the optimum design for a circular channel. A better arrangement would be a thin edge slit which would take advantage of the entire effective length (0.64 cm) of the electron beam. This would be particularly advantageous for the perpendicular arrangement.

It should be noted that if it is not necessary to maintain a minimum pressure, i.e., a minimum temperature, in the inlet system, then a greater sensitivity can be obtained by using a long inlet channel rather than a thin edge orifice. The limiting variable in this case would be the total sample influx that can be handled by the mass spectrometer pumping system. A more directed flow is obtained with a channel and would result in more molecules in the region of the electron beam for the same total mass flow rate through the inlet port.

Calculation of the sensitivity for this case would involve integration over the effective collision covolume where the factor J is included.[5] The integral involved is a very complicated function of L/r and θ would be very difficult to compute.

A qualitative indication of the sensitivity permitted with various channels can be obtained without integrating over the collision covolume. That is, the fraction of molecules, n, entering an inlet channel of finite length which finally emerge within an angle θ with respect to the axis of the channel can be computed from the following integral

$$n = \int_0^{\theta} J \sin 2\theta \, d\theta \qquad (10)$$

where J is the deviation factor discussed above.

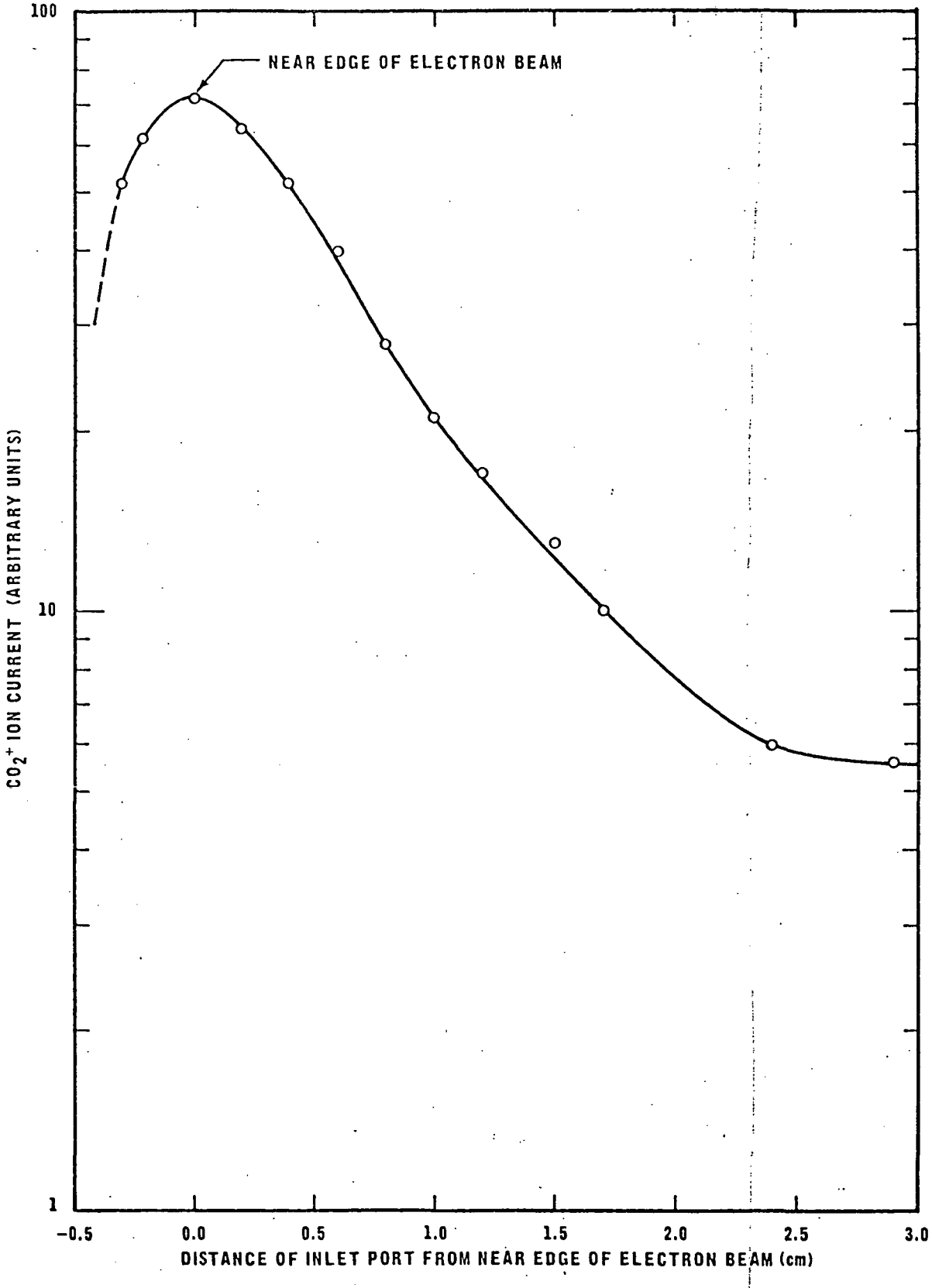

Figure 4. Variation of sensitivity with relative configuration of electron beam and inlet port for the perpendicular arrangement using CO_2 as a test gas.

The value of n has recently been computed numerically and tabulated for numerous values of the parameters L/r and θ.[6] Using these results, the fraction of molecules that actually effuse from the inlet port within an angle θ with respect to the channel axis was calculated and is summarized in Table II. The first row (i.e., for L/r = 0) is for the case of an infinitely thin edge orifice for which J = 1. It is quite obvious from Table II that the flow of sample becomes increasingly more directed in the forward direction for larger values of the length to radius ratio, L/r. For instance, the fraction of molecules emitted within an angle $\theta = 20^{o}$ is more than twice as great for a channel with L/r = 10 than for an infinitely thin orifice. These results indicate that a long exit channel would be quite desirable for experiments in which it is permissible for the cold sample to be maintained at pressures of several torr.

Table II. Fraction of Molecules Effusing From a Cylindrical Channel Within an Angle θ With Respect to the Axis of the Channel.

L/r	20°	30°	40°	50°	60°	70°	80°
0	0.1170	0.2500	0.4132	0.5868	0.7500	0.8830	0.9699
.1	0.1219	0.2594	0.4269	0.6034	0.7670	0.8971	0.9774
.2	0.1267	0.2686	0.4401	0.6188	0.7820	0.9084	0.9817
.5	0.1405	0.2940	0.4749	0.6573	0.8154	0.9272	0.9835
1.0	0.1610	0.3294	0.5185	0.6974	0.8383	0.9311	0.9838
1.2	0.1682	0.3411	0.5313	0.7059	0.8400	0.9315	0.9839
1.5	0.1784	0.3563	0.5461	0.7133	0.8415	0.9321	0.9840
2.0	0.1933	0.3763	0.5609	0.7179	0.8438	0.9332	0.9843
3.0	0.2167	0.3996	0.5721	0.7241	0.8471	0.9346	0.9848
4.00	0.2329	0.4100	0.5787	0.7283	0.8493	0.9352	0.9848
6.00	0.2509	0.4225	0.5871	0.7334	0.8519	0.9364	0.9850
10.0	0.2663	0.4341	0.5949	0.7385	0.8542	0.9373	0.9850

CHAPTER III

RESEARCH RESULTS - CRYOCHEMISTRY

Studies have been conducted on a variety of chemical systems with the general objective of developing new chemistry under the extreme condition of cryogenic cooling. Some new phenomena have been observed. Although the compounds discussed here may seem large, they are not so large as to be meaningless vis a vis the astrophysical questions that are at hand. For example, in the last two or three years, similar compounds have been observed in space by radio astronomy including H_2CO, CH_3OH, NH_3, HCN, HCCCN, HCOOH, CH_3CCH, HNCO, and HNC. Some of these same compounds appear in the following discussion of results from our cryochemical investigations. Some of these compounds also have biological significance, and they are of great concern in exobiology. Mass spectrometric cracking patterns and molecular energetics by electron impact techniques have been the primary means of characterization. In this chapter, we present a cursory summary of these research results.

A. Three Carbon Strained Ring Compounds - Cyclopropene, Cyclopropanone, and Cyclopropenone.

CO_3 is a possible important species in the atmosphere of Mars. We became interested in this compound and in closely related species such as the isoelectronic cyclopropanone. This latter compound would have a higher probability of successful synthesis than would CO_3. These species possess abnormal bonding in the form of small valence angles, and this leads to poor bonding orbital overlap and weak bonds--a condition that is commonly described by the term "ring strain." This abnormal bonding creates a driving force for the molecule to enter into those reactions that would lead to relief of

this strain. Thus, at room temperature, the reactivity may be so great that some molecules exhibit only a fleeting existence. Our interest is in the quench stabilization of such species. The primary effort in this work was to investigate four ring compounds and, from mass spectral and energy measurements at low temperatures, to derive a consistent body of calculated results which would relate such quantities as heats of formation (ΔH_f^o), bond energies (E), bond dissociation energies (D^o), activation energies (ΔH_{act}), and ring strain. Studies at room temperature versus those at low temperatures were used to discern changes in structure, decomposition, etc. with temperature for these reactive molecules. The causes and results of the instability of these molecules would necessarily determine procedures and precautions for their convenient handling. When this work was begun, two of the target molecules, cyclopropanone and cyclopropenone, had never been isolated as pure species and much of the work involved synthesis and separation problems. Cyclopropene, a reactive olefin; cyclopropane, an energetic model for cyclopropanone; and cyclobutanone, a by-product of the cyclopropanone synthesis, were also investigated.

Although it had long been postulated as a reaction intermediate and although it had shown fleeting, but detectable, existence, cyclopropanone had not been isolated as a pure species. Shortly after this work was begun, two papers appeared almost simultaneously, both describing the low temperature synthesis (-78^o) from ketene and diazomethane in solutions of methylene chlorine[7] and liquid propane[8]. These reports on the stability and the polymerization of the reactive product agreed with the results from our study.

In an unusual and unique process, we synthesized cyclopropanone by the direct liquid-liquid, solvent free, reaction of diazomethane and ketene at -145°. This is a synthesis with many novel and interesting facets. It is very unusual to find a liquid-liquid reaction which will proceed at such a low temperature without any external form of activation. The reactor, submerged in a coolant at -145°, quickly conducted away the heat of reaction and prevented the molecule from decomposing. The species had been reported to decompose into CO and C_2H_4 upon its formation in the gas phase[9]. The low temperature also served to slow the rate of cyclopropanone polymerization. The use of low temperatures, pure reagents, and a great excess of ketene led to yields of better than 50 per cent cyclopropanone with the four membered ketone ring, cyclobutanone, as the only side product. Although cyclopropanone can be kept indefinitely at -196°, it appears to begin to slowly polymerize at -90° and reacts so rapidly at room temperature that samples are destroyed within minutes. This reactivity at room temperature causes a severe analysis problem and cyclopropanone can be conveniently studied only at low temperatures.

Although cyclopropanone had been reported to decompose upon its formation in the gas phase reaction of CH_2N_2 and CH_2CO, after quenching to -196°, we found that heating the molecule to room temperature produced no evidence of decomposition or structural changes, but rather an increase in the rate of polymerization. The polymer formed was a white, porous looking solid. The ionization potentials, appearance potentials, and excess energies of the principal ions from cyclopropanone and cyclobutanone were experimentally measured, both over the quenched product and after purification, and their molecular energetics were calculated therefrom. The ionization potentials of cyclopropanone and cyclobutanone were measured to be 9.1 eV and 9.4 eV,

respectively. Both of these values were supported by molecular orbital calculations that were performed in this laboratory and which are discussed later in this report. The important mass spectral and critical potential measurements on cyclopropanone are summarized in Table III. With diazomethane in excess, the reaction products were largely C_4 and some C_5 ketones, but very little of the C_3 ketone. In metal systems which catalyzed the decomposition of CH_2N_2, cyclopropane was observed due to the reaction of CH_2N_2 with its decomposition product ethylene at very low temperatures.

There was also some evidence for the formation of the unknown species allene oxide from the attack of the CH_2 upon the C-O rather than the C-C bond of ketene. Thus,

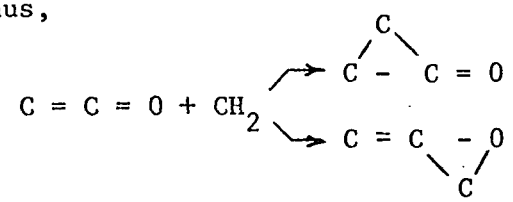

It is also interesting to note that the IP of cyclopropanone is more than an eV lower than that of its open chain isomer acrolein at 10.25 eV. This is due to the increased ground state energy of cyclopropanone plus the decreased energy of its ion due to the ability of the ring to accommodate the positive charge. The appearance potential of $C_2H_4^+$ and CH_2CO^+ are 10.2 and 9.9 eV respectively which are lower than the IP's of the parent species themselves. This again is expected in view of the highly strained (see following discussion) ring system which needs very little energy to break.

Cyclopropene, described in the literature as very reactive and explosive, was investigated both because of this reactivity and as an energetic model for cyclopropenone. It was found to be much easier to handle than one would expect from the literature as it was synthesized,

TABLE III

Summary of Mass Spectral and Critical Potential Data On Cyclopropanone and Its Coproduct Cyclobutanone

m/e	C_3H_4O at -90^{oa}	Appearance Potentials (eV)	C_4H_6O at -70^{oa}	Appearance Potentials (eV)
70			20	9.4
56	15	9.1	3	
42	15	9.9	100	11.0
41	5		14	
39	4		16	
38	4		5	
37	4		5	
36	3		2	
28	100	10.2		13.0
27	35	12.9	12	14.1
26	34	13.5	8	
15				15.7
14		11.6	7	16.7

[a]Temperatures of -90^{o} and -70^{o} for the C_3 and C_4 ketones respectively were levels at which the species exerted convenient vapor pressures in the cryogenic mass spectrometric inlet system. It was however not possible to completely separate the C_3 ketone from the C_4 species due to the similarity of their vapor pressures.

distilled, and transferred at room temperature with no change in structure and with only an insignificant loss from polymerization (which only became noticeable at room temperature). A one week exposure to room temperature destroyed most, but not all of the species. Some dimer was also formed,

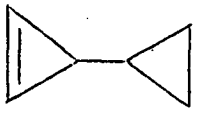

Unfortunately, the mass spectrum of cyclopropene consists of very intense ion peaks corresponding to the positively charged, intact ring and very weak ions resulting from ring fragmentations. The ionization efficiency curves of the weak ion signals were of such poor quality that reliable experimental appearance potentials could not be obtained and hence it was impossible to unambigously develop the molecular energetics. The ionization potential of cyclopropene was measured to be 9.6 - 9.7 eV which was supported by our molecular orbital calculation of 9.6 and close enough to a literature value of 9.95 eV to attribute the differences to experimental errors.

Cyclopropene was studied at -145° and room temperature ($\sim 25^{\circ}$). Although it is known to polymerize at -80° and although the polymerization is believed to be a reaction of the excited double bond diradical[10], no experimentally detected change in the ionization potential (9.6 - 9.7 eV) from -145° to 25° proved that any formation of a triplet species occurs in such small amounts as to be experimentally unimportant.

Cyclopropanone was simiarly studied at -90° and at 25°. Although it was seen to polymerize quite rapidly at room temperature and although many of its reactions in solution are postulated to proceed through the ring

opened dipolar ion (23 kcal/mole more stable than the closed ring[11]), no change in the ionization potential with temperature (9.1 eV) likewise implies no detectable presence of these structures. A difference in structure would, of course, have invalidated physical data taken at room temperature. Mass spectral and energetic data are summarized in Table IV.

According to Breslow [12], the reaction of tetrachlorocyclopropene with tri-n-butyltin hydride at room temperature produces a volatile mixture of chlorocyclopropenes which, when collected in CCl_4 and hydrolyzed with water, produces cyclopropenone in water solution. Breslow postlates the existence of the free ketone, not the gem diol, even in water solution; however, he states that all attempts to separate and isolate the molecule have led to ". . . at least partial polymerization of the compound." He also reports that the ketone may be extracted from water solution by polar solvents and that it is much less reactive and more stable than its saturated analog, cyclopropanone. His paper strongly suggests that cyclopropenone was synthesized and implies that the failure to isolate cyclopropenone was due only to its tendency to polymerize.

Based on our previous work on cyclopropanone and these reactivity statements, we reasoned that cyclopropenone would most certainly be stable enough for cryogenic mass spectrometric analysis once it was separated from its solution. Since it could be extracted, the obvious approach was to find a polar solvent which would allow separation of the ketone at a low enough temperature to prevent polymerization. Although the reported[12] synthesis and nmr analysis for cyclopropenone were reproduced, we were unable to isolate the ketone by any of the following techniques: extraction of the

TABLE IV

Summary of Mass Spectral and Energetic Data on Cyclopropene

m/e	Intensity At -140°	Appearance Potential (eV)
40	60	9.7
39	100	10.9
38	36	
37	23	
36	6.8	
28	< 5	
27	< 2.3	
26	5.7	
15	< 0.6	
14	5.7	
13	< 2.3	

ketone from water solution using different solvents; performing the hydrolysis step in water soluble solvents; partial hydrolysis of the dichlorocyclopropene sample with less than the stoichiometric amount of water; and drying of the solutions to remove dissolved water. We are unable to reasonably explain these failures, and hence we conclude that this very interesting compound must be ascribed as being as elusive as ever.

B. Excess Energy in Molecular Fragmentations.

The literature abounds with examples of fragmentations that contain excess energy. In general, the parent molecular ion contains no excess translational energy and rarely does it contain excess vibrational energy as well. For fragment ions however, the probability of excess energy increases with increase in the number of bonds that are broken. In general, for a molecule R_1R_2 in which $I(R_1) < I(R_2)$, R_2^+ will usually appear with excess energy. Thus we expect at least half of all fragment ions will occur with excess energy. Also we observe that a more abundant fragment ion has less excess energy and vice versa. Thus the ions of low abundance from the necessary breaking of two bonds in the 3-carbon ring compounds will very likely contain excess energy.

Recently a technique for determining excess energy from a peak shape analysis, i.e., based upon the focusing properties of the energetic ions, has been developed for the TOF spectrometer[13]. In addition, this measured kinetic energy of a fragment ion has been rather well correlated with the total excess energy, E^*, in the fragmentation event by the relation,

$$\bar{e}_t = E^*/\alpha N \qquad (11)$$

where α is an empirical constant which was found to be approximately the same for a large number of fragmentation processes in a wide variety of molecules, and N is the number of classical oscillators in the parent molecule. The form of this expression comes from a consideration of the distribution of energy E^* among N classical oscillators. In the fragmentation event,

$$R_1R_2 + e \rightarrow R_1^+ + R_2 + 2e \qquad (12)$$

the excess energy is

$$E^* = A(R_1^+) - \Delta H_r^o \qquad (13)$$

The total translational energy of the fragments, $\bar{e}_t$, is calculated from the measured translational energy of the fragment ion, $\bar{e}_i$, from momentum balance considerations, and the result is

$$\bar{e}_t = \left(\frac{M_i+M_n}{M_n}\right) \bar{e}_i - \left(\frac{M_i}{M_n}\right) (3/2kt) \qquad (14)$$

where M_i and M_n are the masses of the ion and the neutral species from the fragmentation event. From measurements of $A(R_1^+)$ and thus E^* and from measurements of $\bar{e}_i$ and thus $\bar{e}_t$ on a wide variety of molecules, α was found to be very nearly equal to 0.44 for all fragmentations.

A consideration of the ion optics in the Bendix TOF machine leads to the following expression for $\bar{e}_1$

$$\bar{e}_i = (N_o^2/3.69)\ (qE_s)^2\ (W_{1/2}^2/M) \qquad (15)$$

where $\bar{e}_i$ is in eV, N_o is Avogadro's number, q is the charge on the ion, E_s is the ion accelerating potential in the source, $W_{1/2}$ is the peak width at half-height and M is the mass of the ion. The broadening of an ion signal results from the fact that ions are formed in the source with

initial velocities in the direction of acceleration, hence they do not all start from rest, and thus their flight times are different. The method employed here then merely uses the degree of broadening to determine the initial kinetic energy of the ions.

Instrumental factors that affect the intensity of an ion peak in a multiplicative manner did not significantly affect the peak shape. However all of the ion focusing controls were crucial to the measurements.

The excess energies were a function of energy as typically shown in Figures 5 and 6. The data of Figure 5 were reproductions of previous work to authenticate our technique. The curves vary widely in character depending on the potential energy surface of the activated complex. The data of Figure 6 for CH_2^+ from cyclopropane are particularly interesting. Neglecting the rapidly falling data very near the AP, and extrapoling the more gentle higher energy data to the AP yields $\bar{e}_i$ = 0.35 eV and E^* = 103 kcal/mole which is in good agreement with earlier data on this process. Rather if we accept this unusual phenomenon (which we have observed only in these strained ring systems) the energetics can be interpreted by assuming that C_2H_4 and CH_2^+ are produced in excited triplet states. As the bombarding electron energy is increased, some ions are produced as excited triplets with little excess energy while others degenerate to the ground electronic singlet states with the concommitant production of large amounts of excess vibrational and translational energy in the fragments. At some still higher electron energy, almost all of the fragments are produced in the ground electronic states with excess vibrational energy and the upper curve is produced.

The extrapolated excess energies at the appearance potentials for all ions studied here are summarized in Table V. The precision of the data

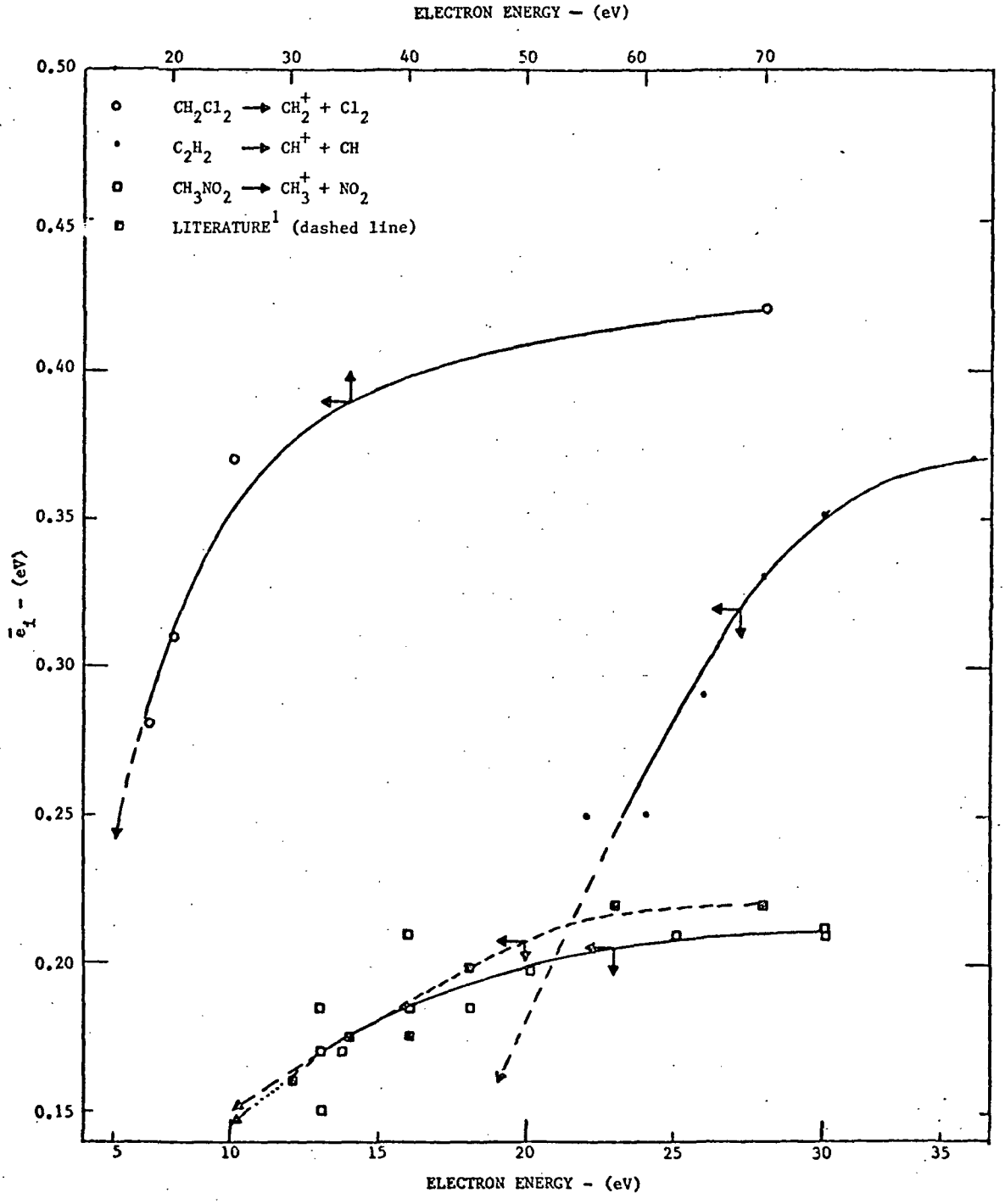

Figure 5. $\bar{e}_i$ Versus Electron Energy for Verification of Experimental Technique

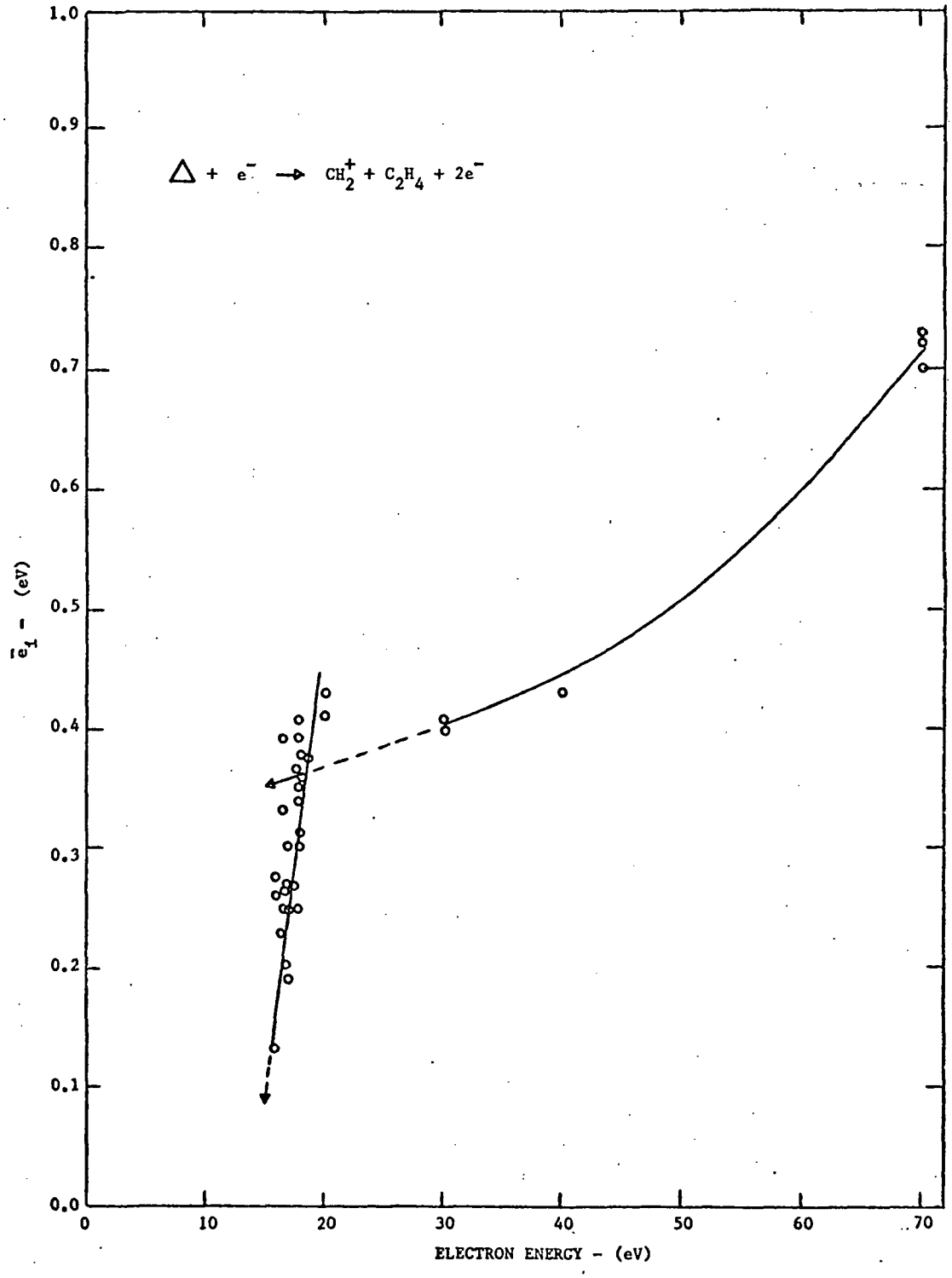

Figure 6. $\bar{e}_i$ Versus Electron Energy for cy-$C_3H_6 \rightarrow CH_2^+$

TABLE V

Summary of Excess Energies (kcal/mole) at AP

for All Compounds Studied in This Research

Parent Molecule	Ion	$\bar{e}_i$	$\bar{e}_t$	E^*	Literature[1] E^*
CH_2Cl_2	CH_2^+	5.5	6.5	28	36
C_2H_2	CH^+	3.7	7.0	21	19
CH_3NO_2	CH_3^+	3.5	4.2	29	29
cy-C_3H_6	$C_2H_3^+$	1.4	2.1	19	21
	$C_2H_2^+$	1.4	1.8	16	15
	CH_2^+	8.0	11.5	103	113
		1.6		18	
	$C_2H_4^+$			--	
	CH_3^+			0	
cy-C_3H_4O	$C_2H_4^+$	1.54	2.2	17	
	$C_2H_2O^+$	1.22	2.2	17	
cy-C_4H_6O	$C_2H_2O^+$	1.53	2.5	26	
	$C_2H_4^+$	1.27	1.7	18	
	$C_2H_3^+$	2.25	3.1	33	
	CH_2^+	2.08	2.3	24	
cy-C_3H_4	CH^+	1.5	1.8	12	
	$C_2H_2^+$	1.25	2.0	13	

1. M. A. Haney and J. L. Franklin, J. Chem. Phys., 48, 4093 (1968).

varies greatly, but the resulting correlated excess energies, E^*, have explained the molecular energetics of this family of strained ring compounds as is evident in the following section of this report.

C. Derived Molecular Energetics.

The molecular energetics of highly reactive cryochemicals is important in understanding both their reaction kinetics and stability characteristics as well as, of course, their thermodynamics. In this research, the molecular energetics were developed by electron impact techniques. One of the major problems in the interpretation of such data is the occurance of energy of excitation in either or both of the ion and neutral fragments in the ionization process itself. The cyclic, strained compounds are a convenient mechanism for the general study of this problem, and the data are, of course also directly applicable to these compounds of astrophysical interest.

In our work, it was found to be very common for the fragments produced upon electron impact of ring compounds to possess excess translational and vibrational energy, but rare for the measured appearance potential to correspond to a fragment in an excited electronic state. This excess energy may be viewed as residual energy from the formation of multiple bonds in the fragments. The introduction of a rearrangement correction term for the energetic difference in the initial and final ring fragmentation products, i.e., the excess energy of the fragmentation process, allowed us to assign ring bond energies to particular bonds and enabled bond dissociation energies and an estimation of ring opening activation energies to be calculated which seem to relate well to literature data from various other kinds of experiments.

Cyclopropane was investigated as an energetic model from which the molecular energetics of cyclopropanone could be discussed. The literature on cyclopropane discusses strain energies, heats of formation, ionization and appearance potential measurements, structure, mechanisms, and reactions. If our mass spectrometric data could be correlated with other existing data for this molecule, a similar and confident interpretation of the new molecule, cyclopropanone, would be possible. The energetics of cyclopropane were successfully explained by the insertion of an energetic rearrangement term, $R(R_1)_g^{ex}$, in the equations for calculating bond energies, $D^o(R_1-R_2^{\cdot})$ and $D^o(R_1^+-R_2)$. This energetic rearrangement term represents the energy difference between a hypothetical initial diradical and the final ground state structure for the fragments which result from breaking two carbon-carbon (C-C) ring bonds. From our measurements with cyclopropane, we were able to calculate the following values (kcal/mole) which compared well with literature data:

$\Delta H_f^o = 13 \pm 3$	(lit. = 12.7)
ring strain = 36	(lit. = 27 relative to paraffins)
E(C-C) = 75	
D^o (C-C) = 52	(lit. = 49)
ΔH_{act} (ring opening) = 65	(lit. = 65)

and wherein the ring strain is localized to the carbon-carbon ring bonds.

Heats of formation in the gas phase of cyclopropanone and cyclobutanone were calculated from our mass spectrometric data to be 27 ± 8 and 13 ± 5 kcal/mole. Bond energies were used to calculate additional ring

strains of 36 and 19 kcal/mole with respect to cyclopropane and cyclobutane, respectively. By a procedure analagous to the one used for cyclopropane, the following values were prediced for cyclopropanone:

$$E(C\text{-}C^{\dagger}) = 66;\ E(C\text{-}C) = 40$$

$$D^{o}(C\text{-}C^{\dagger}) = 45;\ D^{o}(C\text{-}C) = 20$$

$$\Delta H_{act}(C\text{-}C^{\dagger}) = 61;\ \Delta H_{act}(C\text{-}C) = 35$$

It would be quite interesting to predict an activation energy for ring opening at the C-C (rather than the $C\text{-}C^{\dagger}$) bond in cyclopropanone in order to support or dispel the theory that cyclopropanone reactions in solution proceed with a low activation energy via the ring opened dipolar ion. The latter value above supports the theory[11] that cyclopropanone solution reactions do indeed proceed via such a ring opened dipolar ion, but this conclusion is totally dependent upon inclusion of the rearrangment energy term. Without the inclusion of $R(R_1)_g^{ex}$ terms, mass spectrometric results would predict a stronger bond at the distant carbon-carbon bond, $d(C\text{-}C) = 1.58\ \mathring{A}$, than the shorter carbon-carbon bond, $d(C\text{-}C^{\dagger}) = 1.49\ \mathring{A}$. This result particularly points out the necessity of the rearrangement term.

In this work, an experimental procedure was developed to calculate, from mass spectrometric data, the ΔH_f^o for molecules to within about ± 5 kcal/mole. Any lack of precision in the appearance potential and excess energy measurements is partially overcome by using more than one fragment ion to calculate ΔH_f^o. This measurement is only worth the trouble for molecules

---

† carbonyl carbon

with structures from which it is not possible to make a good estimate of ΔH_f^o from other more precise methods. It is particularly adaptable to small rings because the fragments are produced in ground electronic states and correspond to molecules for which ΔH_f^o and ionization potential are usually known and need not be measured. However, it is necessary to check for the occurrence of excess translational and vibrational energies. This technique is simply the reversal of the normal energetic treatment from which the heat of formation of the fragment ion is calculated from the appearance potential by knowing the ΔH_f^o of the parent molecule.

During the course of this work, secondary efforts were needed to develop techniques for the measurement of appearance potentials of ions with long-tail ionization efficiency curves (a more asymptotic-like approach to zero intensity with decreasing electron energy). The determination of critical potentials from ionization efficiency curves that have standard shaped curves (positive slope at zero intensity) is obtainable by any number of methods with varying degrees of precision. These methods include initial break, semi-log matching, retarding potential difference, linear match, and extrapolated difference techniques. On the other hand, the appearance potential of ions with long-tail curves required methods that would separate the curve into sections pertaining to single processes each of which must be interpreted individually. The appearance potential of some of these long-tail, low abundance ions were experimentally undeterminable by any of the above electron impact methods. In any event, by looking for good match of the curves over the first two eV of the curve, one could obtain higher precision and still have a method that emphasizes the initial onset region of the ionization efficiency curve.

An effort was made to apply molecular orbital theory to these ring systems. This work involved no development of molecular orbital theory but merely the application of each of four available computer programs to these ring molecules[a]. Although MO calculations have been performed for some time, it is only in the last few years that new notions, particularly semi-empirical theory, as well as efficient computer programs have been developed which seem to permit the calculation of quantities of chemical interest to within useful accuracies. The four programs used in this work were written by Klopman[14] and Baird[15], both working with M. J. S. Dewar, Pople[16] and Hoffmann[17]. We wished to calculate the ionization potential and heats of atomization (ΔH_a) for comparison with experimental data and to use the molecular orbital theory to help predict the structure of these reactive molecules. For these very reactive species, experimental structure determinations may be a long time forthcoming and it was hoped that mass spectrometric data reinforced by molecular orbital theory could provide some valuable insights. Because of the inability of molecular orbital calculations to predict known molecular structures or even most stable structures from which accurate ΔH_a and ionization potentials could be calculated, theoretical chemists have had to adjust molecular parameters by empirical means such that ΔH_a and ionization potentials could be calculated accurately (on the average)

---

[a]All four programs were obtained from the Quantum Chemistry Program Exchange at Indiana University.

for broad classes of compounds whose actual experimental bond lengths and angles are similar enough to allow a set of "standard" molecular geometries to be used for all molecules in the calculations.

Of the four molecular orbital programs used in this work, the Baird and Klopman programs calculated usable numbers for ΔH_f^o and ionization potentials while only the Pople program appeared to show any promise of structure prediction. Because of the insensitivity of the ionization potential to geometry changes and the good accuracy of calculated versus experimental ionization potentials, the Klopman and Baird programs appear to be usable for calculating ionization potential for cryogenic ring molecules. However, the strong geometry dependence (especially the C-C ring bonds) of both Baird and Klopman programs prevents the use of these two programs for calculating ΔH_f^o until some confidence is gained in assigning standard geometries to abnormal rings. This assignment is further complicated for ring molecules having unmeasured geometries. Although the triplet calculations appear usable for parent molecules, the application to fragments appears to be also dependent on some better understanding of standard geometries. This confidence in assigning standard geometries may be obtainable by working with many known strained rings, or for a particular ring molecule with a family of substituted derivatives of known structure and properties, good agreement may result from calibrating the programs for this family of molecules as has been done for the cyclopropane and cyclopropene families[18]. Once this confidence is gained, the programs offer a strong potential for mass spectrometric identification and distinction

between closed ring and open chain isomers whose ΔH_a and ionization potential usually differ significantly. For very unstable molecules not amenable to nuclear magnetic resonance or infrared analysis, this seems a very worthy goal.

Although parts of the molecular orbital programs may not yet be sufficiently accurate for absolute use, they still offer the possibility of relative comparison of different structures, triplets, isomers, etc. from which qualitative trends or relative quantitative data can be used for mass spectrometric analytic decisions and calculations. Also included in this area is the prediction of relative stabilities of competing products.

D. Cyclobutadiene - The Cyclic Dimer of Acetylene.

Acetylene is a likely cometary constituent and indeed cyanoacetylene (N≡C-C≡CH) has been recently observed in certain regions of space by radio astronomers. This five atom molecule is, of course, strickingly large.

We were thus attracted to a study of cyclobutadiene, which is the 8-atom cyclic dimer of acetylene that had successfully eluded all attempts, many of them very extensive, of synthesis. The molecule was expected to be energetic and intensely reactive. Theoretical calculations have disagreed as to the nature of the ground state of cyclobutadiene, for, depending upon the method of calculation, both singlet and triplet states are predicted. The many experimental failures of synthesis by conventional techniques and the divergent results of theoretical calculations when combined with the seeming relevance of the species in certain astrophysical problems, led us to undertake the synthesis and characterization of cyclobutadiene by our newly developed cryochemical procedures.

Several chemical procedures were explored. An earlier report of indirect evidence for the isolation of cyclobutadiene from the reaction of CIT* with ceric ion at 0° was based on the identification by gas chromatography of very small amounts of methyl benzoate produced by the reaction of the isolated cyclobutadiene with methyl propiolate in the presence of a large amount of cyclobutadiene dimer[19]. This research, reported in 1965 created quite a stir, and it was written up in Chem. and Engineering News. In our research, cyclobutadiene was both liberated from CIT and observed to react immediately with methyl propiolate and other dienophiles upon pyrolysis in the injector of a gas chromatograph. In view of the conditions maintained in the earlier reported experiment[19], the formation of methyl benzoate could be due to this process instead of the assumed reaction of isolated cyclobutadiene with methyl propiolate, and thus this earlier report, though promising, must be discounted accordingly.

We conducted the oxidation of cyclobutadieneirontricarbonyl (CIT) at 0°, the volatile products were transported at 0°, and were then quenched at -180° to -196° in the cryogenic inlet arrangement attached to the mass spectrometer. Upon slow, controlled warming, free cyclobutadiene, was not detected, but cyclobutadiene dimer was observed.

The dehalogenation of cis-3,4-dichlorocyclobutene with sodium amalgam at room temperature followed by immediate quenching of the volatile products at -180° to -196° in the cryogenic inlet system also failed to yield evidence of cyclobutadiene although cyclobutadiene dimer was again observed.

---

*Cyclobutadieneirontricarbonyl

We also attempted the radio frequency discharge of cis-3,4-dichlorocyclobutene at room temperature at pressures of 10^{-1} torr followed by immediate quenching at -196°. HCl, C_2H_2, C_2HCl, C_4H_4, C_4H_2, C_4H_3Cl, and $C_2H_2Cl_2$, were observed upon slow controlled warm-up in the cryogenic inlet system, but the mass spectra and ionization potentials of the C_4 species showed it to be vinylacetylene rather than cyclobutadiene as is evident in Table VI. The C_4 spectrum at -120° has been corrected for the presence of diacetylene, HC≡C-C≡CH, m/e 50, which was produced in the discharge and which revaporized at the same temperature as did the C_4 species. The comparison spectra of Table VI were determined at temperatures of equivalent vapor pressures.

Pyrolysis of CIT was conducted in a specially designed furnace inlet system to the mass spectrometer in which the furnace exhaust was only 1/8 inch from the ionizing electron beam. With pressures of CIT of 10^{-2} to 10^{-1} torr and furnace temperatures of 350° to 400°, cyclobutadiene was produced along with cyclobutadiene dimer, benzene, 1,3-butadiene, vinylacetylene, acetylene, and carbon monoxide. The ionization potential of cyclobutadiene was measured to be 9.3 to 9.4 eV. In the pyrolysis of CIT followed by a rapid quench inside the cryogenic inlet system, C_4H_4 was revaporized and detected at -100°, but the IP was measured to be 9.5 to 9.6 eV as shown in Table VII. Although the mass spectrum and ionization potential of this C_4H_4 species were different from its isomers vinylacetylene and butatriene (see Table VIII) the evidence for the existence of a stable cyclobutadiene at low temperatures was not totally conclusive because of the unavoidable presence of vinylacetylene. The nearness of the ionization potentials and vapor pressures was such that we were never able to measure either the mass spectrum or the IP of the pure species.

TABLE VI

Summary of Important Mass Spectral and IP Data From C_4H_4 Synthesis Experiments With $C_4H_4Cl_2$

m/e	C_4H_4 From rf Discharge of $C_4H_4Cl_2$[a]	Vinylacetylene at -108°	Butatriene at -90°
52	100	100	100
51	59	56	72
50	51	49	51
49	21	19	26
48	7	8	8
39	1	1	1
26	11	12	18
Ionization Potential (eV)	9.7-9.9	9.8-9.9	9.2-9.3

[a]This C_4 species was observed at -120° after quenching the discharge products to -196° followed by slow controlled warm-up for sequential revaporization and analysis.

TABLE VII

Ionization Potentials of C_4H_4 Isomers

Compound	Exp.	Theoretical[c]
cyclobutadiene (singlet)	9.3 - 9.4	8.83, 8.56
cyclobutadiene (triplet)	8.2 - 8.6[a]	8.43
vinylacetylene	9.8 - 9.9 (9.9)[b]	9.60
butatriene	9.2 - 9.3 (9.4)[a]	8.99, 9.16

[a]E. Hedaya, et. al., J. Amer. Chem. Soc., 91, 1875 (1969).

[b]F. H. Field and J. L. Franklin, "Electron Impact Phenomena," Academic Press, New York, New York, 1957, pp. 261.

[c]These theoretical calculations were performed in our laboratory using LCAO-MO-SCF computer programs obtained from the Quantum Chemistry Program Exchange at the University of Indiana.

TABLE VIII

Summary of Important Mass Spectra From CIT Pyrolysis and Quench Experiments

m/e	C_4H_4 from Pyrolysis of CIT[a]	Vinylacetylene at -108°	Butatriene at -90°
52	100	100	100
51	59	56	70
50	51	49	51
49	17	19	26
48	1	9	8
39	5	1	1
26	26	12	18

[a]This C_4 species was observed at -105° after quenching the products from the pyroysis of CIT at 380° to -196° followed by slow controlled warm-up for sequential revaporization and analysis.

The larger percentage of vinylacetylene after the quench accounts for the somewhat higher IP of the revaporized C_4 components. The only other measured IP is for triplet cyclobutadiene produced by the pyrolysis of photo-α-pyrone at 800°C[20]. The agreement with our theoretical value for the triplet is encouraging.

Critical potential measurements on fragment ions sufficient to allow a calculation of the heat of formation of cyclobutadiene were accomplished, but the resulting calculations were inconclusive. Calculations from several perspectives using AP data on several ions yielded values clustered near 30 kcal/mole and near 70 kcal/mole. The discrepancy was probably due to excess energy in the ionization processes, but experimental difficulties prohibited the necessary measurements.

The mechanism of the pyrolysis of CIT was examined. The formation of benzene was evidently due to the reaction of cyclobutadiene and acetylene and not due to the pyrolysis of acetylene. Vinylacetylene was also not due to the pyrolysis of acetylene. The lack of formation of these species from acetylene was demonstrated by blank pyrolysis experiments under the same conditions using only pure acetylene.

Cyclobutadiene was observed to react as expected with dienophiles in the copyrolysis of CIT with methyl propiolate or with dimethyl acetylenedicarboxylate. The reaction of cyclobutadiene with oxygen from the copyrolysis of CIT and oxygen, produced furan. This result agreed with that of flash photolysis of CIT[21] in the presence of oxygen but disagreed with that of the pyrolysis of photo-α-pyrone[20] in the presence of oxygen in which 2-butene 1,4-dione had been produced. The lack of reaction of cyclobutadiene with CH_3 or CH_2 in the copyrolysis of CIT with methyl

bromide or with dibromoethane again suggested that cyclobutadiene produced from CIT had a singlet ground state.

A preliminary account of these results was published, however, because of the remaining uncertainties detailed above, a more complete communication must await further experiments.

E. Cryoquenched Reactions of Oxygen Atoms with Simple Hydrocarbons.

The reactions of oxygen atoms with several simple hydrocarbons followed by rapid quenching to cryogenic temperatures have been studied with the use of low temperature mass spectrometry. The rapid quenching was carried out in an attempt to stabilize the initial reaction products, and the inlet system permitted the detection of any compounds which might be stable only at low temperatures. The systems that were studied were the reactions of oxygen atoms with acetylene, ethylene, and ethane which were 99.6, 99.8 and 99.9 per cent pure respectively as obtained from the supplier, and hence no purification was attempted.

The atoms were produced by means of an efficient radio frequency electrodeless electric discharge arrangement which consisted of a 50-turn copper coil 33 mm O.D. and made of 14 gauge wire. An impedance matching network insured the maximum power transfer from the transmitter to the plasma and hence, maximum production of atomic species. The network was very simple as is evident in Figure 7. The transmitter, operating at 3.5 mHz, had an output impedance of 52 ohms, and hence the network, with its 50 turn coil and plasma core, must be adjusted to 52 ohms. Proper adjustment was indicated by a SWR of near unity. The discharge was self igniting, would operate in pyrex with no cooling, and would maintain an intense discharge

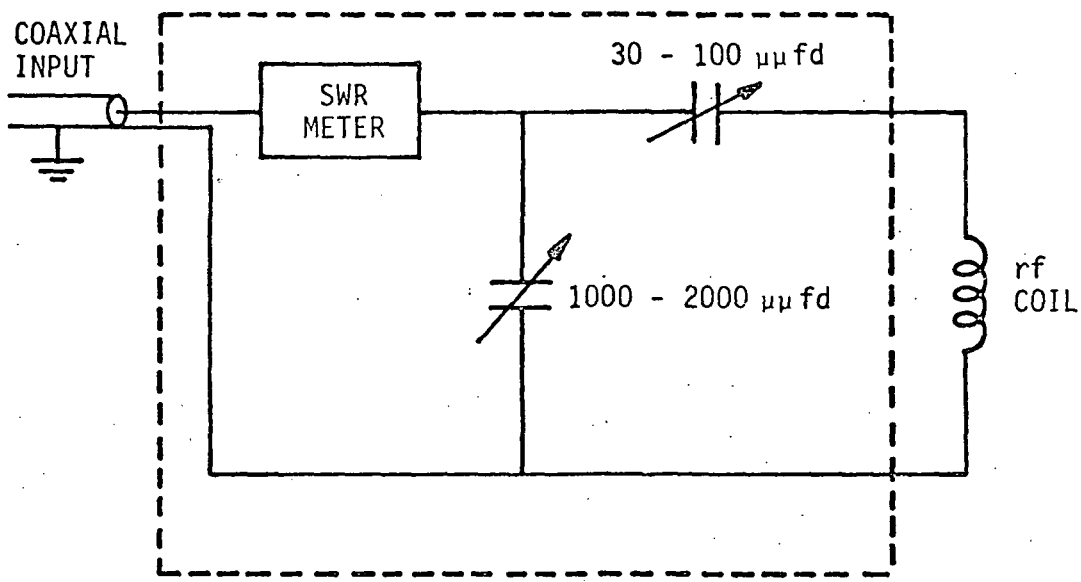

Figure 7. Impedance matching network.

in, e.g., hydrogen at pressures up to 80 torr. Tests for the presence of O and H atoms using the emission from

$$O + NO \rightarrow NO_2 + h\nu$$

and the yellow to blue color change in

$$2H + MoO_3 \text{ (yellow)} \rightarrow MoO_2 \text{ (blue)} + H_2O$$

were always positive, but no attempts at quantitative analysis were ever attempted.

The resulting mixture of atomic O and both ground state and excited molecular O_2 species contacted the second gaseous reactant in a pyrex reactor cooled to very low temperatures, thereby resulting in fast quenching of the reaction products. The quenching temperature was varied from 77^0 to 100^o K and the reactions occurred in a pressure range of 0.5 to 2.5 torr. The low temperatures were produced by immersing the reactor in a dewar of a suitable liquid refrigerant which was stablized with an automatic temperature control system. The reaction products were studied during a controlled warm-up from the quenching temperature by use of the low temperature inlet system.

The reaction of oxygen atoms with ethane followed by a rapid quench to 90^oK produced small amounts of ethanol as the only reaction product in strong contrast to the room temperature reaction which produces CO_2, CO, ethanol, CH_2O, CH_3CHO, and H_2O. These results are an example of a successful attempt to stabilize the initial reaction product by low temperature quenching, and they thus shed light on the reaction mechanism. The reaction probably occurred by an insertion of an excited ^1D oxygen atom into the carbon-hydrogen bond rather than by reaction of the ground state ^3P which would have abstracted an H atom and resulted in a different product array. Unlike the case with either C_2H_4 or C_2H_2, the reaction with C_2H_6 seemed to catalyse the formation of O_3. No O_3 was observed when operating with the lighter

hydrocarbons nor when pumping only discharged O_2-He through the reactor under the same reaction conditions. However, the O_3 formation could have been a physical artifact of the reactor design as well.

The reaction of oxygen atoms with ethylene followed by a rapid quench to 90°K produced products with appearance temperatures as shown in Table IX.

No new or unusual products were observed, and hence these results were first thought to be rather disappointing. However, the presence of relatively large amounts of ethylene oxide supported a proposal by Cvetanovic[22, 23] that the initial reaction product was an energy-rich ethylene oxide molecule. The increased quantities of ethylene oxide produced in the present work was then a result of the low temperature quenching. Formaldehyde, methanol, and formic acid were probably formed from the free radical scavenger action of O_2 that was also present in the reaction zone. These results then are a second example of a rapid quench stabilizing the initial product and thereby giving us insight into the reaction mechanism.

The reaction of atomic oxygen with acetylene followed by a rapid quench to 90°K produced carbon dioxide, glyoxal, formic acid, water, a red compound or complex disappearing at -123°, and a white solid which slowly changed to a yellow and finally to a brown color on exposure to the atmosphere at room temperature. These products and their appearance temperatures appear in Table X. The red color and double C_2H_2 evolution were not reproduced in blank experiments. The red substance was tentatively explained in terms of a charge transfer complex between unreacted acetylene and formic acid wherein the acid proton of the formic acid interacts with

TABLE IX

Products from the Reaction of Discharged Oxygen with C_2H_4 Followed by Quench to 90°K

Temperature Range, °C	Product
-176 to -152	unreacted C_2H_4
-163 to -131	CO_2
-145 to -121	HCHO
-127 to -94	CH_3CHO and CH_2OCH_2*
-82 to -54	CH_3OH
-65 to -10	H_2O
-60 to -10	HCOOH

*The mass specral data permitted a product ratio estimate of acetaldehyde to ethylene oxide of 30:70.

TABLE X

Products from the Reaction of Discharged Oxygen with C_2H_2 Followed by Quench to 90°K

Temperature Range, °C	Evolved Cpd.	Observation
-163 to -135	Unreacted C_2H_2	
-163 to -135	CO_2	
-135 to -116	secondary C_2H_2	red color fading
-103 to -79	O_2	yellow color fading
-82 to -54	$(CHO)_2$	yellow color fading
-50 to -20	HCOOH	
-79 to -20	H_2O	
room temperature		white, fluffy solid

the π electrons of the acetylene. The red color of the complex would be caused by the transfer of electrons from the acetylene to the formic acid. This electron transfer would be to a lower excited state and cause a shift toward longer wavelengths of absorption. This type of absorption is well known, for example, when chloranil (yellow) and hexamethylbenzene (colorless) are mixed, an intensely red solution is formed[24]. In our studies, the proposed charge transfer complex would exist only at low temperatures. Upon warming, the bonding would weaken and the C_2H_2 would be evolved.

We have also found that this same sort of reaction configuration but with benzene rather than C_2H_2 will also yield red deposits at 90°K. Charge transfer complexes of benzene are well known[25].

Glyoxal is yellow, and thus its evaporation would explain the observed color change, but the origin and significance of the accompanying slight O_2 evolution was not established. The room temperature solid was not identified but was found to contain functional groups of aldehydes and esters. Upon exposure to the atmosphere, it gradually became yellow and finally dark brown after about 48 hours. The expected initial reaction product, ketene, was not detected presumably due to the insufficient speed of the quench. $O(^3P)$ does react at 20°K in an argon matrix to yield ketene. Interestingly, $O(^1D)$ would be expected to react with C_2H_2 to form oxiene,

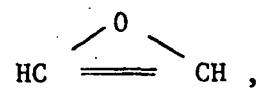

a very strained and presently unknown species. The initial hot species would decompose

$$H_2C_2O^* \rightarrow CO + CH_2$$

$$HCOCH^* \rightarrow CHO + CH$$

and these radicals would react further to form the observed product distribution.

The results obtained from the study of these three reactions indicated that, depending on the molecular complexity and the energetics of the initial reaction products, a variety of intermediates could be stabilized by low temperature quenching.

F. Cryoquenched Reaction of O Atoms with NH_3.

The products of the reaction of atomic oxygen with ammonia with an immediate quench to 90°K are presented in Table XI.

When the O;NH_3 reaction was conducted at room temperature with no quenching, NO and N_2O were the main products. When cooled below -115° the peaks due to these oxides began to decrease indicating that a portion of their precursors were being removed from the reaction zone by the quench. This removal was never completely effective since some NO and N_2O remained even when quenching at 90°K.

The product mass was yellow as previously reported over 40 years ago[26], but the color was due to the normally unstable diimide, N_2H_2, rather than HNO or NH_3O as was then proposed. The color bleached as the N_2H_2 was removed between -125° and -110°. The ionization potential of diimide was measured to be 9.8 ± 0.2 eV in good agreement with a previous value[27].

The AP of $N_2H_2^+$ from N_2H_4 was found to be 11.3 ± 0.2 eV. Hydrazine could have been formed from the dimerization of two NH_2 radicals or from the disproportionation of diimide,

TABLE XI

Products of the Reaction of Discharged Oxygen with NH_3 Followed by Quench to $90^{o}K$

Temperature Range, ^{o}C	Product
-183 to -141	NO
-125 to -110	N_2H_2, N_2, N_2O, unreacted NH_3
-61 to 1	H_2O
-50 to -15	N_2H_4
-1 to > 1	NH_2OH
room temperature	NH_4NO_3

$$2N_2H_2 \rightarrow N_2H_4 + N_2 + 86 \text{ Kcal}$$

which would also explain the evolution of N_2 with the appearance of N_2H_4.

The detection of NH_2OH was important in that it had previously been proposed to exist as an intermediate in the oxidation of NH_3[28]. The compound could have been formed by

$$O + NH_3 \rightarrow NH_2 + OH \rightarrow NH_2OH$$

or by direct insertion. The conversion is exothermic by 119 kcal/mole.

G. Cryoquenched Reaction of H Atoms with NO.

The reaction of hydrogen atoms with nitric oxide followed by a rapid quench to 77°K produced only small amounts of nitrous oxide and water. The expected intermediate, HNO, was not detected; however, the presence of nitrous oxide and water indicated that HNO was produced during the reaction process[29]. The failure to stabilize and detect HNO is supported by a concurrent study made by Robinson[30].

H. Low Temperature Reaction or Ozone and Ammonia.

While discharged oxygen and NH_3 produced a yellow colored product mass upon quenching to 90°K as described above, quenching to 77°K produced an orange-red mass which proved to be formed by the reaction of condensed ozone with the NH_3. In subsequent experiments, a layer of ammonia was condensed on top of a layer of ozone at 77°K. A bright yellow deposit was produced, and as the reactor was slowly warmed, the yellow color changed to a orange-red. In another experiment, the orange-red solid could be formed at 90°K if the discharged oxygen was first forced to strike the liquid oxygen cooled surface before contacting the gaseous NH_3. The preliminary cold wall contact evidently led to ozone,

$$O + O_2 + M \rightarrow O_3 + M$$

The orange-red solid bleaches at -70^{o} and white solid NH_3NO_3 is produced. Ozone and oxygen appear over a wide temperature range of -153^{o} to -112^{o} during slow warming. Thus we conclude that the original product was NH_4O_3 which decomposed according to

$$2NH_4O_3 \rightarrow NH_4NO_3 + 1/2O_2 + 2H_2O$$

This proposal is in keeping with earlier related observations[31,32].

I. The Lower Boron Hydrides.

Borane, BH_3, should be a stable species at sufficiently low temperatures, as should, for that matter, BH as well. The simplest known boron hydride is diborane, B_2H_6, which is itself a very energetic and uniquely bonded molecule. And BH_3 and BH should be even more energetic. Thus the objective here was the identification and determination of the energetics of these molecules by mass spectrometric techniques, and an attempt to prepare each as a stable liquid or solid phase by utilization of cryogenic reactor techniques. A secondary effort was made to produce H_2BF in order to obtain more information concerning unstable trivalent compounds of boron.

The boron hydrides, particularly B_2H_6, and also the higher alkylated boranes had received considerable attention because of their parctical usefulness, especially as rocket and jet aircraft fuels. In addition, much interest and controversy has been focused upon the unusual bonding present in these compounds due to their so-called "electron deficient" nature.

Initial attempts to detect BH_3 in the pyrolysis of B_2H_6 and dimethylanilineborane involved the introduction of the pyrolysis products into the ionization region of the mass spectrometer by effusion through small diameter orifices. This approach had been used successfully in this laboratory in the study of CF_2[33] as well as in other investigations of unstable molecules and free radicals[34]. However, BH_3 could not be detected in a lengthy and sometimes frustrating series of hot filament and tubular furnace pyrolysis experiments. When BH_3 was finally observed by introducing the pyrolysis products directly into the electron beam without the presence of a beam collimating orifice, it became clear that future investigations of unstable species should be conducted, if possible, in this manner. Whereas CF_2 was not lost upon effusion through a 0.032 inch diameter orifice[33], BH_3 suffered decomposition or reaction under similar experimental conditions.

A radio frequency discharge of B_2H_6 failed to produce evidence of BH_3. If BH_3 were actually formed in the discharge, it would have been depleted by the time the discharge products reached the ionization region of the mass spectrometer approximately one foot away. This became apparent only later during the cryogenic quenching experiments when it was found that BH_3 could not be successfully transferred through a 1-1/2 foot long by 3/8 inch diameter tube which had been cooled over its entire length to a temperature approximately that of the melting point of oxygen ($54.8^{\circ}K$).

BH_3 was finally detected successfully in the pyrolysis of B_2H_6 in tubular furnaces of quartz, aluminum, and stainless steel at pressures of 10^{-4} to 10^{-2} torr and at temperatures of 250° to 400°. BH_3 was also produced by the pyrolysis of B_2H_6 on incandescent filaments of platinum,

tungsten, nichrome, zirconium, molybdenum, niobium, titanium, and tantalum. The ionization potential of BH_3 was determined by two independinet methods to be 12.32 ± 0.1 eV. By comgining this with a value of 14.88 ± 0.05 eV for $A(BH_3^+)$ from B_2H_6, $D(BH_3 - BH_3)$ was calculated at 2.56 eV or 59 kcal/mole.

The appearance potentials of B^+, BH^+, BH_2^+, BH_3^+, and $B_2H_5^+$ from B_2H_6, as well as from BH_3 wherever applicable, were determined. Although several of these values are in major disagreement with other studies, the numbers presented are considered to be accurate because of the experimental precision, and the excellent self-consistency of the resulting numbers. The latter is demonstrated by three determinations of $D(BH_3 - BH_3)$ as approximately 2.6 eV from the appearance potentials of three separate fragment ions. All of the appearance potential data from B_2H_6 and BH_3 are summarized in Table XII.

The experimental appearance potentials permitted the direct determination of either the values of or the lower and/or upper bounds for $D(B^+ - H)$, $D(BH^+ - H)$, $D(BH_2^+ - H)$, $D(BH_3 - BH_3)$, $D(BH_3^+ - BH_3)$, $I(B_2H_6)$, and $I(B_2H_5)$. The calculation of $D(B - H)$, $D(BH - H)$, $D(BH_2 - H)$, and $I(BH_2)$ was made possible by introducing the spectroscopic value of $I(BH) = 9.77$ eV[35]. The values are consistent with some of the data from spectroscopic, kinetic, and mass spectrometric studies and also are upheld by theoretical arguments in several cases. These calculated energetic quantities are summarized in Table XIII.

The utilization of the derived bond energies to calculate the heat of formation of B_2H_6 as -40.9 kcal/mole at 298° K allowed an analysis of the errors in the experimental bond energies from this research. This was accomplished by comparing the calculated heat of formation from our data with an experimental value of 7.53 kcal/mole[36] which is believed to

TABLE XII

Appearance Potentials of Fragment Ions from BH_3 and B_2H_6

Fragment Ion	Appearance Potential from Parent in eV (This Work)[c]		Appearance Potential from Parent in eV (Literature)		
	BH_3	B_2H_6	BH_3	B_2H_6	
B^{10+}	15.83[a]	18.39 ± 0.02		18.7 ± 0.1[d]	19.5 ± 0.2[e]
$B^{10}H^+$	13.66 ± 0.02[b]	16.39 ± 0.3		14.9 ± 0.1	16.6 ± 0.2
$B^{10}H_2^+$	12.95 ± 0.05	15.5 ± 0.05		13.4 ± 0.1	13.5 ± 0.5
$B^{11}H_3^+$	12.32 ± 0.1	14.88 ± 0.05	11.4 ± 0.2[f]	13.1 ± 0.2[g]	12.1 ± 0.2[g]
$B^{11}{}_2H_5^+$		11.84 ± 0.1		11.9 ± 0.2	11.3 ± 0.5
$B^{10}H_6^+$				11.9 ± 0.1	12.1 ± 0.2
$B^{10}{}_2H_5^+$				11.9 ± 0.1	12.0 ± 0.3

[a]Calculated as $A(B^+)$ from B_2H_6 or (18.39 eV) minus $D(BH_3 - BH_3)$ or 2.56 eV.

[b]Error represents maximum deviation from average of experimental values.

[c]Average of experimental values.

[d]W. S. Koski, et. al., J. Amer. Chem. Soc., 80, 3202 (1958).

[e]J. L. Margrave, J. Phys. Chem., 61, 38 (1957).

[f]T. P. Fehlner and W. S. Koski, J. Amer. Chem. Soc., 86, 2733 (1964).

[g]Fragment ion is $B^{10}H_3^+$.

TABLE XIII

Bond Energies and Ionization Potentials Calculated or Estimated from Appearance Potential Measurements

Bond Energy or Ionization Potential	Energy, eV		
		Literature	
	This Research	Experimental	Calculated or Estimated
$D(B - H)$	3.64	< 3.51[35]	3.39[a], 3.40[b]
$D(BH - H)$	4.83		4.7[c]
$D(BH_2 - H)$	3.58	3.2[d]	3.2[c]
$D(B^+ - H)$	2.17	< 2.04[35]	3.0[c]
$D(BH^+ - H)$	5.23		5.2[c]
$D(BH_2^+ - H)$	0.63		0.9[c]
$D(BH_3 - BH_3)$	2.56	1.7[d], > 2.39[e]	1.23[h], 1.61[i] 2.25[j], < 1.66[k]
$D(BH_3^+ - BH_3)$	< 3.67; > 3.04		
$I(B_2H_6)$	< 11.84; > 11.21	11.9[f], 12.1[g]	
$I(BH_2)$	9.37	9.8[d]	8.2[c]
$I(B_2H_5)$	> 8.26		7.86[f]

[a] A. C. Hurley, Proc. Royal Soc. (London) Ser. A., 261, 237 (1961).
[b] F. O. Ellison, J. Chem. Phys., 43, 3654 (1965).
[c] W. C. Price, et al., Discussions Faraday Soc., 35, 201 (1963).
[d] T. P. Fehlner and W. S. Koski, J. Amer. Chem. Soc., 86, 2733 (1964).
[e] E. J. Sinke, et al., J. Chem. Phys., 41, 2207 (1964).
[f] W. S. Koski, et al., J. Amer. Chem. Soc., 80, 3202 (1958).
[g] J. L. Margrave, J. Phys. Chem., 61, 38 (1957).
[h] R. E. McCoy and S. H. Bauer, J. Amer. Chem. Soc., 78, 2061 (1956).
[i] T. P. Fehlner and W. S. Koski, ibid., 87, 409 (1965).
[j] R. P. Clarke and R. N. Pease, ibid., 73, 2132 (1951).
[k] M. E. Garabedian and S. W. Benson, ibid., 86, 176 (1964).

be a correct number. This calculation involved $D(BH_3 - BH_3)$, the heat of sublimation of boron, the dissociation energy of hydrogen, and two times the value of the heat of atomization of BH_3. If all values except the latter are assumed to be accurate, it may be seen that an error of 24.2 kcal/mole in the heat of atomization of BH_3, i.e., $D(BH_2 - H) + D(BH - H) + D(B - H)$, would produce the rather large disagreement between the two heats of formation. That is, an average error of approximately 8 kcal/mole or 0.35 eV exists in the derived bond energies of BH, BH_2, and BH_3. This is believed to be the case as opposed to assigning what would be a considerable error to $D(BH_3 - BH_3)$. The errors are not believed to be due to the experimental appearance potential values, but to be inherent in the electron impact method of energy determinations, e.g., Franke Condon problems.

Free BH_2 was not detected in the pyrolysis of B_2H_6 even though the experimental conditions under which BH_2 was reportedly synthesized in earlier studies in another laboratory were essentially reproduced[37].

Equilibrium partial pressures calculated from free energies of reaction based on the bond energies from this research and entropy values from estimated thermodynamic tables showed that the pyrolysis of B_2H_6 should produce approximately equal amounts of BH_2 and BH_3. However, by again employing the experimental bond energies, the magnitudes of the activation energies for the dissociation of B_2H_6 into BH_2 and into BH_3 were estimated and a comparison of the resultant kinetic rate constants indicated that BH_2 would not play a significant role in the kinetics of the pyrolysis of B_2H_6.

The quench of the products of the pyrolysis of B_2H_6 in the cryogenic reactor inlet system at temperatures as low as approximately the melting point of oxygen (54.8°K) failed to produce evidence of stabilized BH_3. That is, BH_3 was not observed either by monitoring the pyrolysis and quenching operation or by monitoring the gas evolved from the deposit upon warm-up. However, the observation of an increase in the H_2^+ ion peak at approximately 60°K followed by a decrease in its intensity at higher temperatures led to the initial conclusion that BH_3 had been stabilized at the quenching temperature, but was reacting or decomposing to liberate H_2 as the temperature of the system was increased. This concurred with an earlier x-ray detection of an unidentified phase with a triple point of 60°K in the quenched products of a microwave discharge of B_2H_6[38]. A subsequent blank experiment in which unpyrolyzed B_2H_6 and H_2 were subjected to the cryogenic quench produced the same variation of the H_2^+ ion peak upon warm-up. The final conclusion was that H_2 was trapped in the B_2H_6 matrix and liberated at approximately 60°K.

H_2BF was not detected in similar cryogenic quenching experiments in the products of an rf discharge of BF_3 and B_2H_6. However, HBF_2 was observed upon warm-up of the quenched discharge products to about 90°K. The lowering of $A(BF_2^+)$ to approximately 13 eV was evidence that HBF_2 and not BF_3 was the parent compound since $A(BF_2^+)$ from BF_3 is 16.2 eV[39]. Also, the appearance of HBF^+ and BF_2^+ peaks at a temperature slightly lower than that at which peaks from BF_3 begin to appear agreed with the reported similarity of the vapor pressures of HBF_2 and BF_3[40]. Finally, the

approximate 1:1 ratio of m/e ion peaks 31 and 49 concurred with a mass spectrometric study of HBF_2[40].

CHAPTER IV

SUMMARY LISTS

A. Graduate Theses

1. "Mass Spectrometric Study of the Products Obtained from Fast Cryogenic Quenching of Several Reactions Involving Atomic Hydrogen or Atomic Oxygen"

   Author: D. B. Bivens
   Degree: Ph.D. in Chemical Engineering

2. "Synthesis, Stability and Energetics of Cylobutadiene"

   Author: P. H. Li
   Degree: Ph.D. in Chemical Engineering

3. "Synthesis and Mass Spectra of Cyplopropene and Cyclopropenone"

   Author: M. A. Bell
   Degree: M.S. in Chemical Engineering

4. "The Preparation of Some Highly Reactive, Three Membered Ring Organic Compounds as Cryochemical Reagents, and the Low Temperature Mass Spectrometric Study of Their Stability and Molecular Energetics"

   Author: R. J. Holt
   Degree: Ph.D. in Chemical Engineering

5. "Mass Spectrometric Studies of the Synthesis, Energetics, and Cryogenic Stability of the Lower Boron Hydrides"

   Author: J. H. Wilson
   Degree: Ph.D. in Chemical Engineering

B. Publications

1. "A Refrigerated Inlet Arrangement for Mass Spectrometric Studies of Unstable Species at Cryogenic Temperatures, " Rev. Sci. Instr. 37, 561 (1966), T. J. Malone, W. J. Martin and H.A. McGee, Jr.

2. "Low Temperature Synthesis," Chem. Eng. Prog. 62, 113 (1966), D. B. Bivens, T. J. Malone, J. H. Wilson and H. A. McGee, Jr.

3. "Mass Spectrometric Studies of the Synthesis, Energetics, and Cryogenic Stability of the Lower Boron Hydrides," J. Chem. Phys. 46, 1444 (1967), J. H. Wilson and H. A. McGee, Jr.

4. "Mass Spectrometry in Cryochemistry," presented at 157th National ACS Meeting, Minneapolis, April, 1969 and reviewed in Chem. and Eng. News, 47, No. 17, 50 (1969), H. A. McGee, Jr.

5. "Mass Spectrum and Ionization Potential of Condensed Cyclobutadiene," Chem. Comm., 592, 1969, P.H. Li and H. A. McGee, Jr.

6. "Cryochemical Technology," Cryog. Technol., 7, 109 (1971), R. J. Holt and H. A. McGee, Jr.

7. "Cryochemical Synthesis of Cyclic Three Carbon Compounds", J. Am. Chem. Soc., in press, R. J. Holt and H. A. McGee, Jr.

8. "Molecular Energetics in Highly Strained Three Carbon Ring Compounds", R. J. Holt, H. A. McGee, Jr., and E. F. Rothgery, in preparation.

REFERENCES

1. Donn, B., in Formation and Trapping of Free Radicals, A.M. Bass and H. P. Broida, editors, Academic Press, New York, N.Y., 1960. See also B. Donn, Icarus 2, 396 (1963).

2. Damoth, D. C., Advances in Analytical Chemistry and Instrumentation, Vol. 4, edited by C. N. Reilley, Wiley, New York, N.Y., 1965.

3. Biemann, K., Mass Spectrometry Organic Chemical Application, McGraw-Hill, New York, N.Y., 1962.

4. Blanchard, L. P., and P. LeGoff, Can. J. Chem. 37, 515 (1959).

5. Clausing, P., Z. Physik. 66, 471 (1930).

6. Miller, A. N., J. Chem. Phys. 42, 3734 (1965).

7. Turro, N. J. and W. B. Hammond, J. Amer. Chem. Soc. 88, 3672 (1966).

8. Schaafama, S. E., H. Steinberg, and Th. J. DeBoer, Rev. Trav. Chem. 85, 1170 (1966).

9. Kistiakowsky, G. B. and K. Lauer, J. Amer. Chem. Soc. 78, 5699 (1956).

10. Wiberg, K. B. and W. J. Bartley, ibid. 82, 6375 (1960).

11. Turro, N. J., Acc. Chem. Res. 1(2), 33 (1969).

12. Breslow, R., and G. Ryan, J. Amer. Chem. Soc. 89, 3073 (1967).

13. Franklin, J. L., P. M. Hirl and D. A. Whan, J. Chem. Phys. 47, 3148 (1967).

14. Dewar, M. J. S., and G. Klopman, J. Amer. Chem. Soc. 89, 3089 (1967).

15. Baird, N. C. and M. J. S. Dewar, J. Chem. Phys. 50, 1262 and 1275 (1969).

16. Pople, J. A. and G. A. Segal, ibid. 44, 3289 (1966).

17. Hoffman, R., ibid. 39, 1397 (1963).

18. Baird, N. C. and M. J. S. Dewar, J. Amer. Chem. Soc. 89, 3966 (1967).

19. Watts, L., J. D. Fitzpatrick and R. Pettit, J. Amer. Chem. Soc. 87, 3253 (1965).

20. Hedaya, E., et al., ibid. 91, 1875 (1969).

21. Tyerman, W. J. R., et al. Chem. Comm. 497 (1967).

22. Cvetanovic R. J., J. Chem. Phys. 23 1375 (1955).

23. Avramenko L. I., and R. V. Kolesnikova, Zhur. Fiz. Khim. 30, 581 (1956).

24. Murrell, J. N., Quart. Rev. 15, 191 (1961).

25. Hassel, J., Mol. Phys. 1, 241 (1958).

26. Geib, K. H. and P. Harteck, Ber. 66B, 1815 (1933).

27. Foner, S. N. and R. L. Hudson, J. Chem. Phys. 28, 719 (1958).

28. Anderson, J. H., Biochem. J. 95, 688 (1965).

29. Clyne, M. A. A., Tenth Symposium on Combustion, Combustion Institute, Pittsburgh, 1965, p. 311.

30. Field, F. H. and J. L. Franklin, Electron Impact Phenomena, Academic Press, New York, N.Y., 1957, p. 278.

31. Solomon, I. J., et al., J. Amer. Chem. Soc. 84, 34 (1962).

32. Herman, K. and P. A. Giguere, Can. J. Chem. 43, 1746 (1965).

33. Martin W. J. and H. A. McGee, Jr., J. Phys. Chem. 76, 738 (1968).

34. Lossing F. P., Mass Spectrometry, edited by C. A. McDowell, McGraw-Hill, New York, New York, 1963.

35. Bauer, S. H. et al., J. Mol. Spectry. 13, 256 (1964).

36. Gunn, S. R., and L. G. Green, J. Chem. Phys., 36, 1118 (1962).

37. Fehlner, T. P. and W. J. Koski, J. Amer. Chem. Soc. 87, 409 (1965).

38. Bolz, L. H., et al., J. Chem. Phys. 31, 1005 (1959).

39. Law, R. W. and J. L. Margrave, ibid. 25, 1086 (1956).

40. Lynds, L. and C. D. Bass ibid. 43, 4357 (1965).